Added value of an atmospheric circulation pattern based statistical downscaling approach for daily precipitation distributions in complex terrain

Brian Böker, Patrick Laux, Patrick Olschewski, Harald Kunstmann

Angaben zur Veröffentlichung / Publication details:

Böker, Brian, Patrick Laux, Patrick Olschewski, and Harald Kunstmann. 2023. "Added value of an atmospheric circulation pattern based statistical downscaling approach for daily precipitation distributions in complex terrain." *International Journal of Climatology* 43 (11): 5130–53. https://doi.org/10.1002/joc.8136.

Received: 21 November 2022 | Revised: 9 May 2023 | Accepted: 25 May 2023 | Published on: 10 June 2023

DOI: 10.1002/joc.8136

RESEARCH ARTICLE

International Journal of Climatology RMetS

Added value of an atmospheric circulation pattern-based statistical downscaling approach for daily precipitation distributions in complex terrain

Brian Böker[1] | **Patrick Laux**[1,2] | **Patrick Olschewski**[1] | **Harald Kunstmann**[1,2]

[1]Institute of Meteorology and Climate Research (IMK-IFU), Karlsruhe Institute of Technology, Garmisch-Partenkirchen, Germany

[2]Institute of Geography, University of Augsburg, Augsburg, Germany

Correspondence
Brian Böker, Institute of Meteorology and Climate Research (IMK-IFU), Karlsruhe Institute of Technology, Campus Alpin, Kreuzeckbahnstrasse 19, 82467 Garmisch-Partenkirchen, Germany.
Email: brian.boeker@kit.edu

Funding information
Bundesministerium für Bildung und Forschung

Abstract

Reliable prediction of heavy precipitation events causing floods in a world of changing climate is crucial for the development of appropriate adaption strategies. Many attempts to provide such predictions have already been conducted but there is still much potential for improvement left. This is particularly true for statistical downscaling of heavy precipitation due to changes present in the corresponding atmospheric drivers. In this study, a circulation pattern (CP) conditional downscaling to the station level is proposed which considers occurring frequency changes of CPs. Following a strict circulation-to-environment approach we use atmospheric predictors to derive CPs. Subsequently, precipitation observations are used to derive CP conditional cumulative distribution functions (CDFs) of daily precipitation. Raw precipitation time series are sampled from these CDFs. Bias correction is applied to the sampled time series with quantile mapping (QM) and parametric transfer functions (PTFs) as methods being tested. The added value of this CP conditional downscaling approach is evaluated against the corresponding common non-CP conditional approach. The performance evaluation is conducted by using Kling–Gupta Efficiency (KGE), root mean squared error (RMSE), and mean absolute error (MAE) metrics. In both cases the applied bias correction is identical. Potential added value can therefore only be attributed to the CP conditioning. It can be shown that the proposed CP conditional downscaling approach is capable of yielding more reliable and accurate downscaled daily precipitation time series in comparison to a non-CP conditional approach. This can be seen in particular for the extreme parts of the distribution. Above the 95th percentile, an average performance gain of +0.24 and a maximum gain of +0.6 in terms of KGE is observed. These findings support the assumption of conserving and utilizing atmospheric information through CPs can be beneficial for more reliable statistical precipitation downscaling. Due to the availability of these atmospheric predictors in climate model output, the presented method is potentially suitable for downscaling precipitation projections.

KEYWORDS
bias correction, circulation patterns, ERA5, extreme events, heavy precipitation, simulated annealing, statistical downscaling

1 | INTRODUCTION

Heavy rainfall from convective systems and the resulting pluvial floods are common phenomena during the summer season in Central Europe. According to the European Severe Weather Database (ESWD, 2022) over 6000 such events have been reported for the last 70 years in Germany. Heavy rainfall events have the potential to cause severe damage to people, infrastructure, and buildings in the affected areas. In particular, the year 2021 featured extraordinary heavy precipitation events and pluvial floods (e.g. Ahrtal flood in Western Germany). According to the German Insurance Association (GDV 2021) 2021 has been the single most expensive year for insurance dealing with natural hazards that are especially linked to the heavy rainfall events in Western Germany. As stated in MunichRE (2022) the total costs of these events amounted to 33 billion Euro. The events in 2021 are just one example and there are many more described in literature (e.g. Grieser et al., 2006; Piper et al., 2016).

It is well known that precipitation is linked to the state of the atmosphere and therefore to the synoptic circulation which is prone to changes due to ongoing global climate change. In parts of Germany trends in heavy precipitation occurrence have already been described in literature (e.g. Deumlich & Gericke, 2020; Warscher et al., 2019). Since these trends are already present it is necessary to account for them in the future. In the planning of flood protection, for example, it is common practice to construct technical measures in a way they are able to withstand events with a certain return level, for example, the return level of a 100-year flood or heavy precipitation event. The distribution of precipitation in a specific area may shift due to the effects of climate change. Therefore it is crucial to derive information about the magnitude of these expected changes for developing adaption strategies (Rözer et al., 2016). In order to derive qualitative values for possible changes in the distribution of precipitation and therefore return levels and return periods in the future, it is common practice to use the output of dynamic atmospheric models for predictions. The Intergovernmental Panel on Climate Change (IPCC) developed a set of plausible future scenarios which include relevant drivers for the changes in the atmospheric system like the emission of greenhouse gases (IPCC, 2021). These scenarios can be used to drive global circulation models (GCMs) and nest regionally specific regional climate models (RCMs) into them. The approach of nesting models is used for dynamical downscaling which yields atmospheric variables on a higher spatial resolution (Giorgi et al., 2009). However, for the assessment of precipitation return levels on a local scale, other appropriate approaches are needed since GCMs in particular but also RCMs have biases in variables like precipitation (Ibebuchi, 2022). Nevertheless, the general skill in simulating the large-scale and intermediate-scale circulation of GCMs and in particular RCMs is widely accepted (Ibebuchi, 2023; Sunyer et al., 2015). Such an appropriate approach can be statistical downscaling utilizing circulation pattern conditional downscaling as applied in Bárdossy and Pegram (2011) and Lutz et al. (2012). Circulation pattern-based approaches are well established throughout the climate sciences and are considered skillful in projecting surface variables such as temperature and precipitation (Bárdossy & Pegram, 2011; Ramos et al., 2015). For the creation of suitable circulation pattern classifications in general two approaches can be distinguished. The first approach is 'environment-to-circulation' which considers the targeted variable (e.g. precipitation) in the classification process. The other approach is 'circulation-to-environment' whereas the classification process only considers predictors (e.g. sea level pressure) to derive classes (Dayan et al., 2012).

This study follows a strict 'circulation to environment' approach and all circulation patterns are created solely from atmospheric predictors like mean sea level pressure or geopotential. Plenty of different clustering methods are described in literature (e.g. Laux et al., 2020; Philipp et al., 2007). Of the available methods, the optimization method Simulated Annealing and Diversified Randomization (SANDRA) is a promising selection for clustering atmospheric data. SANDRA is able to overcome the shortcoming of getting stuck to local optima compared to the widely used k-means clustering method and its performance is deemed equivalent to self-organizing maps clustering (Philipp et al., 2016). Many studies (e.g. Bárdossy & Pegram, 2011; Jacobeit et al., 2017; Laux et al., 2020; Wilby et al., 1998) conclude that the state of the atmosphere represented by circulation patterns can be linked to surface variables like precipitation and have discriminative power for deducting transfer functions potentially suitable for statistical downscaling of precipitation. The followed approach of using only atmospheric variables as predictors without taking the precipitation into consideration for the clustering opens up the opportunity to assign the identified circulation patterns to

RCM scenario simulation output with ease. This makes it possible to build catalogues of daily atmospheric states in the future for different scenarios. However Faranda et al. (2020) and Demuzere et al. (2009) conclude that major changes in future atmospheric patterns are present in terms of occurrence probability, predictability, and persistence. This needs to be taken into consideration when attempting to attribute future precipitation to future circulation patterns. Nevertheless according to Horton et al. (2015) and Shepherd (2014) the assumption that the internal variability of circulation patterns remains stationary meaning that there will not be completely new patterns in the future is justified. These considerations are essential for the aim of this study. The objective of this study is in presenting a circulation pattern (CP) conditional downscaling approach which conserves the information of changes described by Demuzere et al. (2009) and Faranda et al. (2020) in circulation pattern frequency changes and utilizes this additional information for refined precipitation downscaling to the station level. Due to this additional information, the downscaled precipitation is assumed to be more accurate in terms of the complete precipitation distribution and in terms of the representation of extremes than using a common statistical downscaling approach. The proposed method is evaluated against the latter and the added value is investigated. Circulation patterns created using atmospheric predictors only can be assigned to climate model output with ease. Therefore the proposed circulation pattern conditional downscaling approach may provide the opportunity of deriving sophisticated precipitation information while accounting for circulation pattern frequency changes if applied to future scenario runs.

2 | STUDY REGION

As the study region, we selected the German region Bavarian Oberland (simply referred to as Oberland from here on) situated between Munich in the North and Austria in the South which is formed by the four counties of Weilheim-Schongau (WM), Garmisch-Partenkirchen (GAP), Bad Tölz-Wolfratshausen (TÖL) and Miesbach (MB) (Figure 1). The Oberland covers an area of 3956 km^2 and features a distinct topographic division into two areas of different geographic properties. The northern half can be characterized as an undulating prealpine landscape mostly formed by vast glaciers during the last glacial period. The southern half on the other hand is part of the Bavarian Alps and is considered a mountainous area. Especially in the Western part, it is characterized by high alpine areas featuring complex topography with alternating valleys and mountain ridges as well as peaks reaching 2000 m above sea level and higher. The Oberland is one of the areas having the highest amounts of annual precipitation in Germany. Additionally, it has a high occurrence of heavy precipitation events which frequently result in pluvial floods. Due to the presence of measurement sites set up more than 200 years ago, the region has a comparatively high density of reliable long-term precipitation observations available. According to Deumlich and Gericke (2020) and Warscher et al. (2019) the Oberland has shown increasing trends in precipitation during the past and is continuing to do so in the future. The combination of diverse terrain in a relatively small area, the high occurrence frequency of heavy precipitation events, and the good availability of data fit well with the aims of this study.

3 | DATA AND METHODS

3.1 | Data

The datasets used for this study can be distinguished into two groups. First, ERA5 reanalysis data was obtained from the European Centre for Medium-Range Weather Forecasts (ECMWF). Second, observation data from the German Weather Service (Deutscher Wetterdienst—short DWD) covering the same period as the used ERA5 data. This data was used for the model training as well as model evaluation. All the datasets used are described in more detail in the subsections below.

3.1.1 | ERA5 reanalysis

ECMWF's ERA5 reanalysis dataset is the newest implementation of ECMWF reanalysis datasets which have widely been used as a gridded data source for training and evaluation purposes concerning atmospheric variables and circulation pattern analysis. In these studies, ERA5 is frequently described as a superior reanalysis product and is therefore the dataset of choice in this study (e.g. Kučerová et al., 2017; Mahto & Mishra, 2019). The ERA5 dataset provides a huge variety of variables on pressure levels as well as surface variables on a 0.25° spatial resolution. All variables are available globally though for this study only a specific subdomain and specific variables have been selected. The years 1980–2019 were selected from the available daily ERA5 data. The analysis period of this study is therefore 1980–2019. The obtained predictors were mean sea level pressure, geopotential at 500 hPa, and the u-and v-wind components at 10 m. For in-depth information about the characteristics of the ERA5 product see Hersbach et al. (2020).

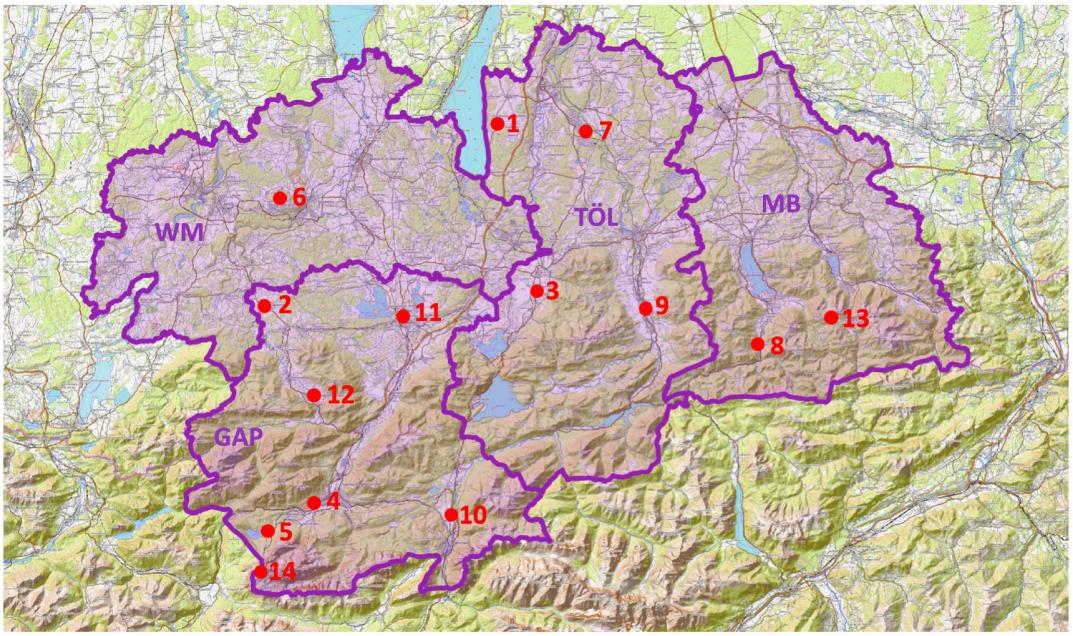

FIGURE 1 The Bavarian Oberland region in southern Germany. The four counties of Weilheim-Schongau (WM), Garmisch-Partenkirchen (GAP), Bad Tölz-Wolfratshausen (TÖL), and Miesbach (MB) forming the Oberland are highlighted in purple. Red dots indicate the location of the measurement sites used in this study. Red numbers correspond to number used in Table 1.

3.1.2 | DWD stations

Reliable precipitation observations for the selected study region are obtained from the German Weather Service (Deutscher Wetterdienst, 2022). These station observations are used on a daily time resolution in consistency with the ERA5 data. Dependent on the measurement site the covered time periods of the measurements may vary greatly, nevertheless due to the limited temporal availability of ERA5 reanalysis data the used station data is bound to the same time constraints. Out of all the available stations within the study area only those stations have been selected that have data available for the whole study period lasting from 1980 to 2019. These considerations lead to the 14 selected stations listed with their key characteristics in Table 1. Their spatial distribution throughout the study region is shown in Figure 1.

3.2 | Methods

Figure 2 gives an overview of the applied model chain. This study follows a two pathways approach in the sense of performing a standard downscaling of precipitation to station level (the outer right vertical path in Figure 2) as a reference and a circulation pattern conditional downscaling (the left vertical pathway in Figure 2) as assumed more skillful approach. The latter takes additional information about the state of the atmosphere (circulation patterns derived from ERA5 reanalysis data) into consideration for downscaling. Finally, the performance of the approaches can be assessed relative to each other by comparison of suitable evaluation metrics. All steps will be described in detail in the corresponding sections following.

Predictor, domain selection and time selection

The selection of predictor variables is key to the creation of skillful circulation patterns which have sufficient discriminative power concerning precipitation to provide beneficial information for CP conditional downscaling. In this study, only three combinations of the vast possible set of variables are tested but these are assumed suitable for several reasons. The first variable used is mean sea level pressure (MSL) which is known to be one of the main drivers of formations bearing precipitation in the mid-latitudes and its predictive skill has been proven by other studies beforehand (e.g. Bárdossy & Pegram, 2011). The second set of variables consists of mean sea level pressure and geopotential at 500 hPa (MSL + z500). This combination has been chosen to be able to compare the created classification to the general circulation patterns by Hess and Brezowsky as described in Gerstengarbe and Werner (2005) that are broadly used to describe atmospheric states influencing Central Europe and are based on expert's analysis of said variables. The third tested set of variables is a combination of mean sea level pressure

TABLE 1 Station numbers, IDs, names, coordinates and altitude.

Number	ID	Name	Longitude (*E*)	Latitude (N)	Altitude (m)
1	217	Attenkam	11.364282	47.877428	670
2	318	Bad Bayersoien	10.995599	47.691926	812
3	349	Benediktbeuren	11.413941	47.706327	630
4	1550	Garmisch-Partenkirchen	11.062126	47.482989	719
5	1734	Grainau-Eibsee	10.993872	47.456150	1008
6	2290	Hohenpeißenberg	11.010819	47.800869	977
7	2674	Geretsried	11.477530	47.843312	608
8	2740	Kreuth-Glashütte	11.646185	47.610509	897
9	2943	Lenggries	11.582626	47.679998	698
10	3307	Mittenwald-Buckelwiesen	11.265311	47.477866	984
11	3424	Murnau	11.223842	47.668879	624
12	3677	Oberammergau	11.060714	47.602966	832
13	4617	Obere Firstalm	11.854407	47.670059	1368
14	5792	Zugspitze	10.984761	47.421037	2965

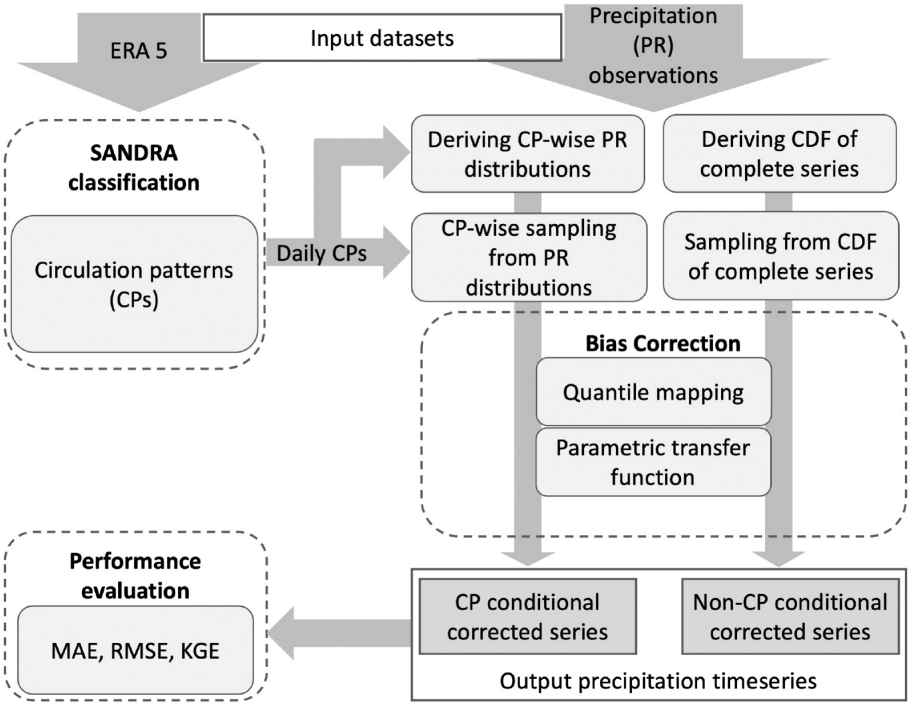

FIGURE 2 Schematic of the applied methods. CDF stands for cumulative distribution function.

and the u- and v-wind components at 10 m (MSL + 10 m wind). According to Liu et al. (2013) the wind direction influences the spatial distribution of precipitation directly due to valley interactions with near surface level atmosphere caused by the complex topography in the study area. Therefore the inclusion of surface wind components is tested due to the assumption of being superior to the first two combinations.

The extent of the domain is selected considering smaller domain sizes as desirable in terms of initial computational expenses and representation of more region-specific characteristics. Nevertheless, the domain should be large enough to not only cover the study region itself but allow for the inclusion of important geographic features of the surrounding area (e.g. the Alps, the northern Adriatic sea, and the Gulf of Genova). Since the search for the best-fitting domain size can be challenging and is not the focus of this study the final extent of the domain is selected within the constraints described above. The domain used stretches from 42°N to 51°N and

6°E to 15°E (note that the given boundary coordinates correspond to the centres of the boundary grid cells). Using this domain the mentioned geographic features are included, the study region is well in the centre, and the size of 37 times 37 grid cells is still fairly small.

The available time period for the study has been selected as described in the previous section. The period from 1980 to 2019 has been split into a 35-year training period from 1980 to 2014 and a subsequent evaluation period from 2015 to 2019. For this study, an extended summer season, June, July, August, and September (JJAS) is taken into consideration. Due to the used daily data and the described boundaries, the resulting training period contains 4270 days and the evaluation period 610 days.

SANDRA classification

SANDRA is short for **S**imulated **AN**nealing and **D**iversified **RA**ndomization, a clustering method developed by Philipp et al. (2007). This method has been selected since it has been applied for circulation pattern analysis yielding good clustering results in terms of explained cluster variance in several other studies (e.g. Laux et al., 2020; Lutz et al. (2012)). Additionally, the SANDRA algorithm is able to overcome shortcomings of conventional optimization methods like k-means. Clustering data having local optima using conventional methods can lead to ambiguous results since there are no strategies implemented to avoid these local optima. The design of the SANDRA algorithm addresses this issue so the global optimum can be reached reliably. To achieve this SANDRA allows for wrong cluster assignments of data objects at each iteration if the acceptance probability $\underline{p}$ is higher than a randomly generated number between 0 and 1.

$$p = \exp\left(\frac{D_{\text{old}} - D_{\text{new}}}{T}\right) \tag{1}$$

D_{new} is the Euclidean distance between the data object and the new cluster and D_{old} is the Euclidean distance to its present cluster. T is a parameter called temperature control parameter that is set to high values at initialization and decreases with each iteration i. The increment of decrease of the temperature is controlled by a cooling factor C.

$$T_{i+1} = CT_i \tag{2}$$

The high initial temperature values allow for relatively free movement of the data objects at the start, therefore, giving the opportunity to check out a lot of different possibilities and slowly reach convergence at the global optimum as the temperature parameter and therefore the freedom of movement of data objects decreases. Due to the need for very slowly decreasing temperatures to ensure reaching the global optimum and therefore unacceptable long run times of the procedure, the diversified randomization technique is applied. The latter performs the simulated annealing process 1000 times but only the first one with the cooling factor set comparably close to 1 and the following 999 runs with significantly faster cooling rates and selects the best run in the end. Philipp et al. (2007) show that this combination of simulated annealing and diversified randomization performs as well as single runs with very slow cooling rates but at reduced computational costs. In order to compare the performance of different runs -both internally while running a SANDRA classification as well as externally with different predictors or numbers of classes—the explained cluster variance (ECV) is used. The ECV is defined as:

$$\text{ECV} = 1 - \frac{\text{WSS}}{\text{TSS}} \tag{3}$$

where WSS is the so-called within-cluster sum of squares and TSS is the total sum of squares. The WSS value can be considered as an internal cluster coherence metric and the TSS value as an external cluster coherence metric. To achieve high internal and low external coherence it is desirable to have low WSS and high TSS values resulting in high ECV values. More in-depth information about the SANDRA algorithm is given in Philipp et al. (2007). Additional to the ECV as a clustering performance metric, the cluster internal RMSE between days assigned to a cluster and cluster centroids are calculated (Figure A1 in Appendix). This provides an additional instance of assessment of statistical assignment quality of days matching their corresponding cluster centroids. As mentioned the ECV can be used to compare the quality of clusters based on different predictors but additionally, the ECV can be considered a function of the number of clusters. This relation can be seen in Figure 3. In general, more clusters lead to a higher ECV. In order to avoid extensive cluster number criteria testing, the desired number of clusters follows the approach of being as small as possible while having clusters with an ECV of 0.8 for the best predictor combination (MSL + 10 m wind). Though this has a subjective component it is considered satisfying because the optimization of ECV is not the goal of this study. Considering this the chosen solution is one of seven clusters for all variables used.

In order to conduct a circulation pattern conditional sampling as described later for the evaluation period it is necessary to assign the found cluster centroids to the part of the ERA5 dataset leftover for evaluation generating a daily cluster catalogue for this period. To do so an

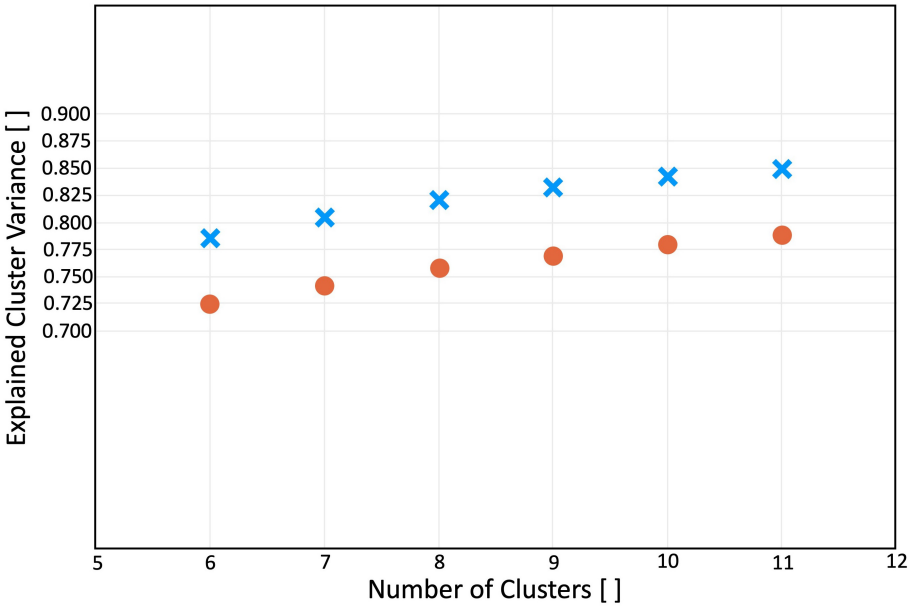

FIGURE 3 Explained cluster variance as a function of the number of clusters for mean sea level pressure combined with u and v wind components at 10 m (crosses) and mean sea level pressure combined with geopotential at 500 hPa (circles) as predictors.

assignment based on the Euclidean Distance is conducted with the cost733class ASC function. Further details on the ASC function can be found in Philipp et al. (2014).

Linking circulation patterns to precipitation

To be able to take advantage of the additional information the circulation patterns may provide for sampling and correcting precipitation it is necessary to statistically link the states of the atmosphere to the precipitation typical for this state of the atmosphere at a specific location. A very common approach for the representation of the distribution of precipitation values is the calculation of their cumulative distribution function (CDF). CDFs can be calculated for the complete available precipitation time series which gives an idea of the overall distribution of precipitation values in this time series (e.g. from a specific measurement site). However, it is equally possible to calculate CDFs dependent on certain boundary conditions such as considering only values in a time series with a distinct CP present. The latter calculation gives the opportunity to calculate the CDFs for every CP separately and therefore distinguish relatively wet or dry CPs. If the assumption that CPs can have discriminative power concerning precipitation, what has already been shown by Bárdossy and Pegram (2011) and Laux et al. (2020) the separately calculated CDFs provide a CP conditional set of CDFs for the subsequent precipitation sampling. In this study, these considerations are implemented in a way that for each of the 14 stations, one single CDF of the complete training period is calculated for conducting the standard approach and a set of 7 CDFs of CPs for the CP conditional approach.

Sampling and bias correction

Due to the evaluation period being considered as a 'test case future projection' without observations, daily precipitation series need to be generated before bias correction can be applied. To do so various methods like weather generators (e.g. Kilsby et al., 2007), Markov-Chain models, or fitting distributions (e.g. Liu et al., 2011) are available. For this study, a simple approach of fitting distributions and sampling from them has been selected. According to Maity et al. (2019) exponential functions belong to the group of best-fitting distributions in the study area. In the first step an exponential distribution

$$f(x;\theta)=\frac{1}{\theta}e^{-\frac{x}{\theta}} \tag{4}$$

with scale parameter θ is fitted to the observed daily precipitation during the training period. In the second step, the actual precipitation time series generation is conducted by drawing a random sample from the fitted distribution for each day of the time series. Steps one and two are executed for every station so a distinct precipitation time series for each station is modelled.

Modelling precipitation in general inherits multiple sources of uncertainties as described in (e.g. Eden et al., 2012; Gudmundsson et al., 2012) which leads to biases between modelled and observed precipitation. To address these biases and to improve the agreement of modelled and observed precipitation it is common practice to conduct bias correction. Numerous different methods are available to achieve this task which varies in their correction performance depending on which target

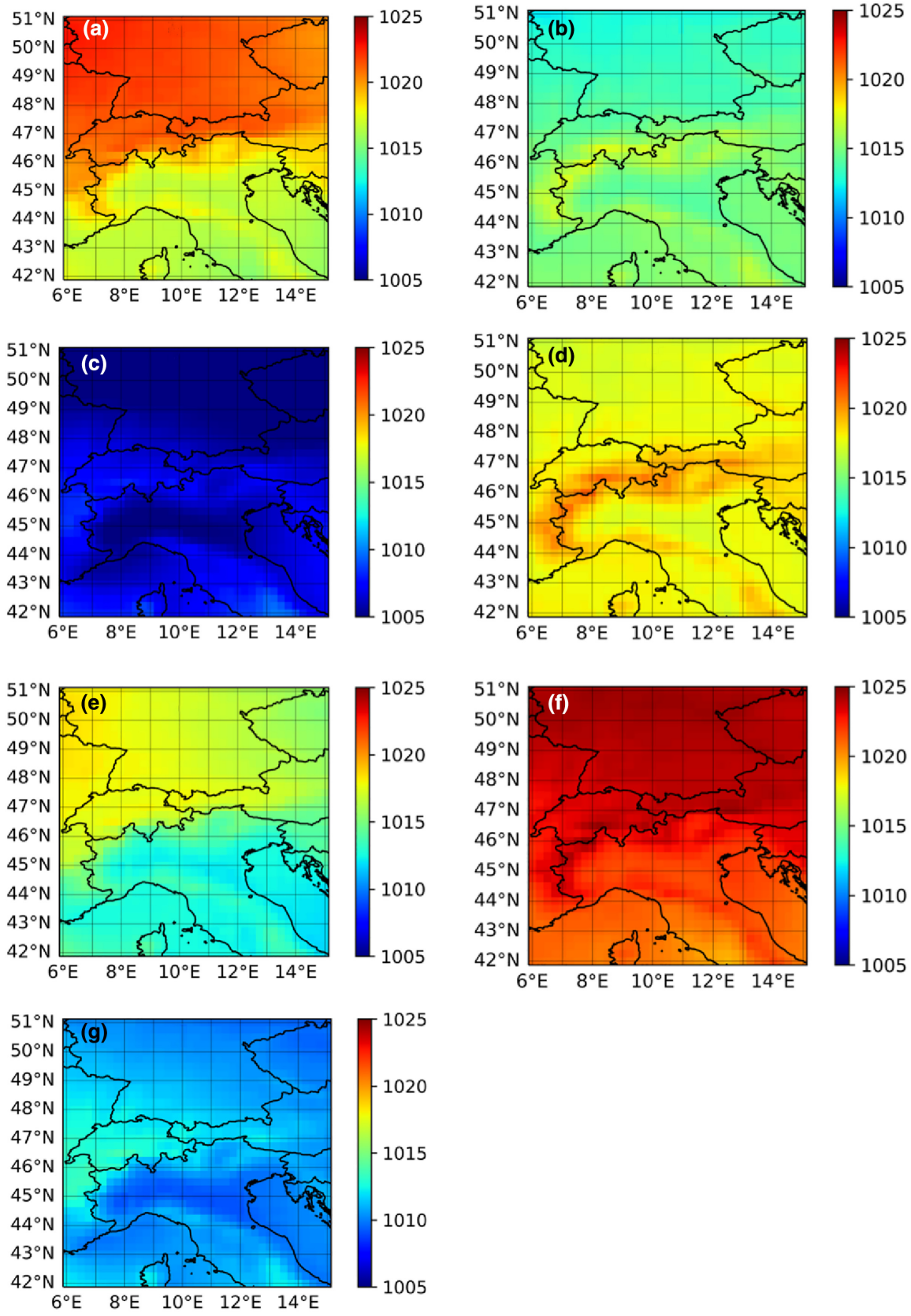

FIGURE 4 Mean sea level pressure (hPa) cluster centroids of a 7 cluster CP 1–CP 7 (a–g) solution based on mean sea level pressure and u and v wind components ERA5 data.

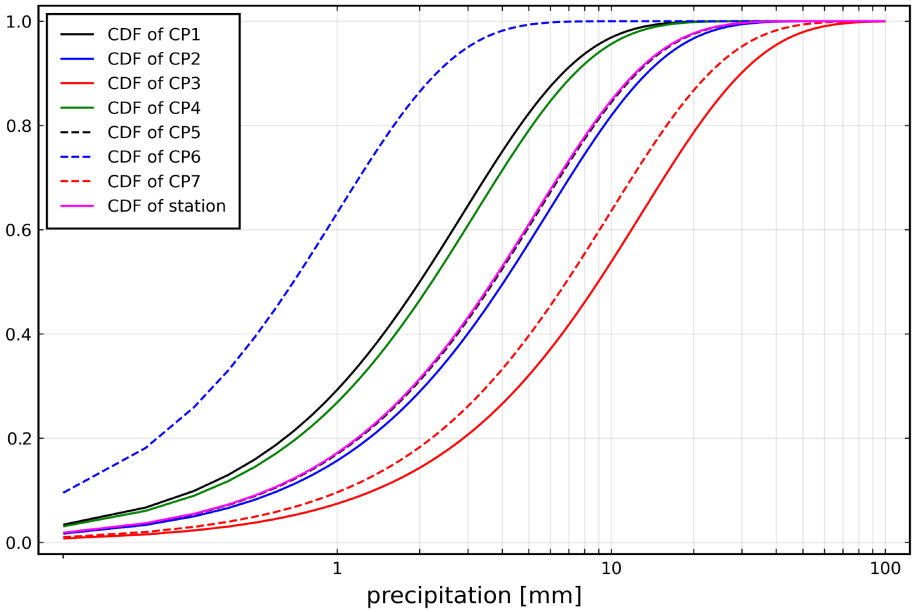

FIGURE 5 Circulation pattern conditional cumulative distribution functions of the 7 cluster solution based on mean sea level pressure and u- and v-wind component at Garmisch-Partenkirchen station. The CDF of the station for all days is given as reference.

variable (temperature, precipitation, wind, etc.) needs to be corrected (Gudmundsson et al., 2012). Gudmundsson et al. (2012) conclude that non-parametric transformations have a superior performance over parametric methods in correcting precipitation biases independent of underlying distribution assumptions. Therefore the statistical bias correction method of choice for this study is the non-parametric transformation empirical quantile mapping which is described by Boé et al. (2007) and in the following is simply referred to as 'QM'. For the purpose of evaluating the influence of correction method choice, a parametric transformation has been selected as an additional method. Both methods are well established and widely used (e.g. Boé et al., 2007; Eden et al., 2012; Gudmundsson et al., 2012; Piani et al., 2010). As described in Gudmundsson et al. (2012) and Piani et al. (2010) these methods are suitable to find a transfer function f which can be used to solve

$$x_{\mathrm{cor}} = f(x_{\mathrm{mod}}) \tag{5}$$

where x_{cor} is the corrected variable and x_{mod} is the modelled variable. The notable difference of the applied methods is therefore the way how the transfer function f from a given set of training data is derived.

According to Boé et al. (2007) QM uses the cumulative distribution function (CDF) of a training simulation and the CDF of the observations to derive a quantile-based transfer function. In the next step, the correction function is applied to the biased modelled output variable to correct it quantile by quantile. The practical application of the QM approach in this study follows Boé et al. (2007). Percentiles are corrected and in between two percentiles a linear interpolation is applied. Since the variable to be corrected in this study is precipitation the occurrence of drizzle effects is addressed by ensuring the probability of precipitation after the correction matches the observed probability of precipitation. For values exceeding the upper boundary of the correction function, a simple extrapolation is conducted so a constant correction value is applied which equals the correction value for the highest quantile.

The second applied bias correction method uses a linear transfer function instead of empirical quantiles. As proposed in Piani et al. (2010) the relation between the corrected variable x_{cor} and the modelled variable x_{mod} can be described as

$$x_{\mathrm{cor}} = a + b x_{\mathrm{mod}} \tag{6}$$

with a being an additive and b an multiplicative correction parameter. The transfer function is completely described by these two parameters giving it the form of a linear function and belongs to the category of parametric transfer functions. In the following, it is simply referred to as 'PTF'.

One of the key features of this study is to contrast the standard bias correction approach using only the precipitation data as correction information to a CP conditional approach using the CPs as additional information for the correction. The latter draws its inspiration from Bárdossy and Pegram (2011). However, the conducted CP conditional approach is modified in a significant way to be able to compare the standard method to the CP conditional method directly. For the standard approach, one CDF fitted to the whole precipitation distribution of the

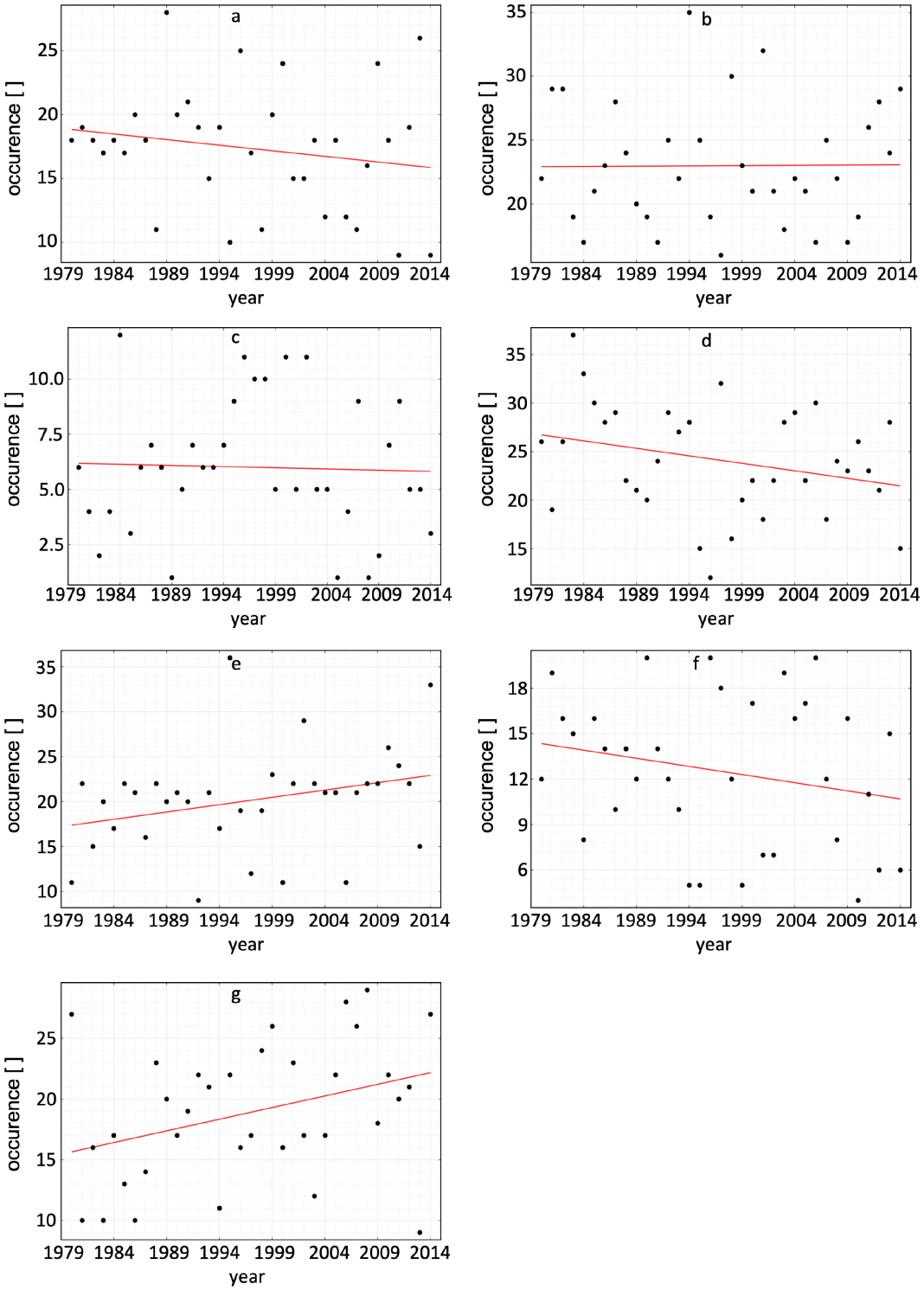

FIGURE 6 1980–2014 frequency changes in the occurrence of the 7 circulation patterns described in Section 4.1.

training period is used for the raw sampling of the evaluation period time series. Subsequently, the described bias correction methods are applied to the raw time series. In contrast to that the CP conditional approach uses a set of fitted CDFs, one for each CP occurring in the training period and samples dependent on the CP present on a specific day in the evaluation period from the corresponding CDF (e.g. if a day of the evaluation period has CP 4, the sample for that day will be drawn from the CDF of CP 4, etc.). This leads to the generation of as many time series as CPs are present and each time series contains as many days as the corresponding CP

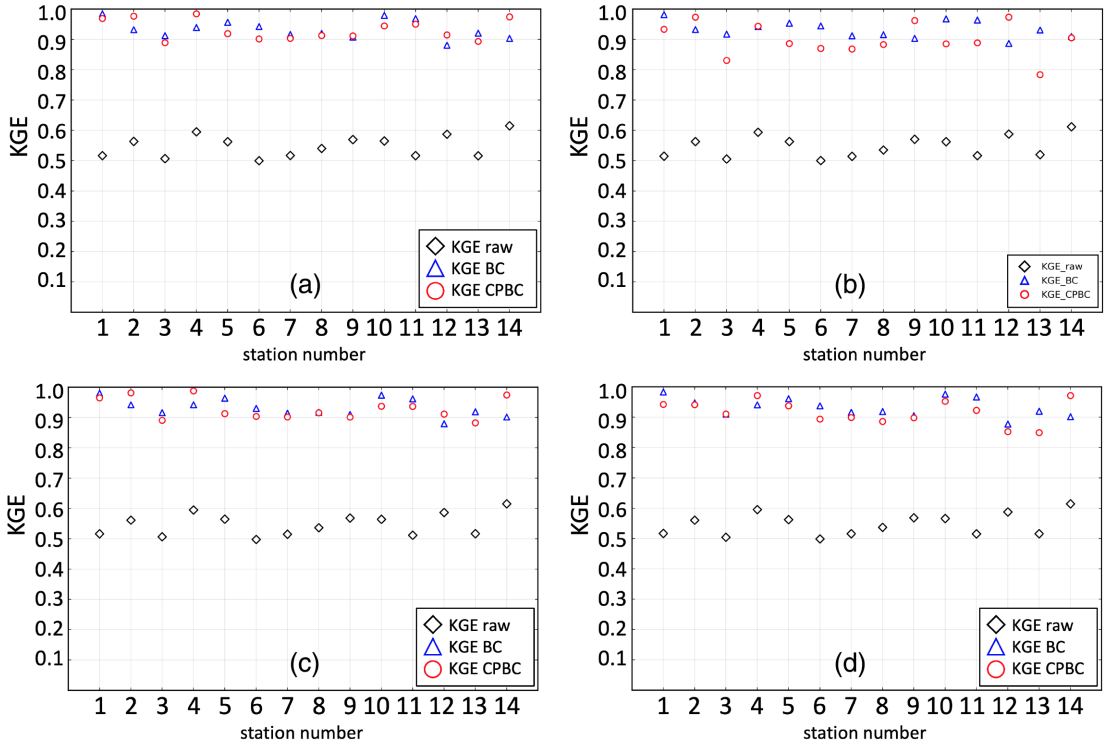

FIGURE 7 Kling–Gupta efficiency at all stations with different classifications. Used predictors for the classifications are mean sea level pressure (a), mean sea level pressure and geopotential at 500 hPa (b), mean sea level pressure and 10-meter u- and v-wind component (c), Hess-Brezowsky general circulation patterns (d). (a–c) are 7-cluster solutions and (d) is a 30-cluster solution. Black diamonds indicate uncorrected model output, blue triangles corrected model output by standard method, and red circles CP conditional corrected model output.

occurred in the evaluation period. Each CP conditional time series is then corrected separately. In the end, the time series for the whole evaluation period is created by merging the CP conditional time series. To ensure the stability of the described models all steps are repeated 500 times. The output time series ready for evaluation is generated by calculating the mean of the sorted separate time series, once for the standard method and for the CP conditional method.

Evaluation metrics

For performance evaluation of applied precipitation downscaling methods numerous different metrics are available. Of these, two commonly used metrics used in this study are mean absolute error (MAE) and root mean square error (RMSE). The calculation is conducted by applying the equations given in Chai and Draxler (2014):

$$\mathrm{MAE}=\frac{1}{n}\sum_{i=1}^{n}|e_i| \tag{7}$$

$$\mathrm{RMSE}=\sqrt{\frac{1}{n}\sum_{i=1}^{n}e_i^2} \tag{8}$$

with n samples of errors e_i and $i=1,2,\ldots,n$. In accordance with Chai and Draxler (2014), a combination of metrics is often required, and therefore both metrics are used in parallel in this study. Also due to this, the Kling–Gupta model efficiency (KGE) is used as an additional performance assessment metric. Originally described in detail in Gupta et al. (2009) the KGE is calculated as:

$$\mathrm{KGE}=1-\sqrt{(r-1)^2+(\alpha-1)^2+(\beta-1)^2} \tag{9}$$

with r being the linear correlation between observations and simulations, α a measure of variability error and β the mean bias term. According to Knoben et al. (2019) α can therefore be calculated as the quotient of standard deviation in simulations and standard deviation in observation:

$$\alpha=\frac{\sigma_{\mathrm{sim}}}{\sigma_{\mathrm{obs}}} \tag{10}$$

While β is calculated as the quotient of the simulation mean and the observation mean:

$$\beta = \frac{\mu_{sim}}{\mu_{obs}} \quad (11)$$

4 | RESULTS

4.1 | Classification

4.1.1 | Circulation patterns

The resulting circulation pattern centroids of the chosen seven cluster MSL + wind solution are shown in Figure 4, the centroids of the MSL + z500 solution are shown in Figure A1. The MSL centroids shown in Figure 4 are suitable for a brief description and interpretation of the general state of the atmosphere. CP 1 can be described as a pattern with a distinct separation between the central European part north of the Alps and the Mediterranean part south of the Alps with higher pressure dominating the northern part and pressure levels close to the standard pressure present in the southern part. CP 5 belongs to the same group of patterns with such a clear separation along the Alps and a higher pressure scheme in the northern part but not as dominant as in the case of CP 1, with the southern part being closer to standard pressure. CP 2, 3, 4, and 6 can be grouped as patterns without this clear distinction between parts of the domain. The main difference between the patterns is the general pressure level present in them with CP 3 being a strong low-pressure pattern, CP 6 being a strong high-pressure system and CP 2 and CP 4 being in between with CP 2 around standard pressure, and CP 4 having a weak high-pressure pattern. CP 7 however forms its own group being a pattern of generally low pressure with a distinct higher-pressure wedge present in the western part of the domain. Investigating the occurrence of heavy precipitation events under certain CPs, it has to be noted that for precipitation events in the 99th percentile P 3, CP

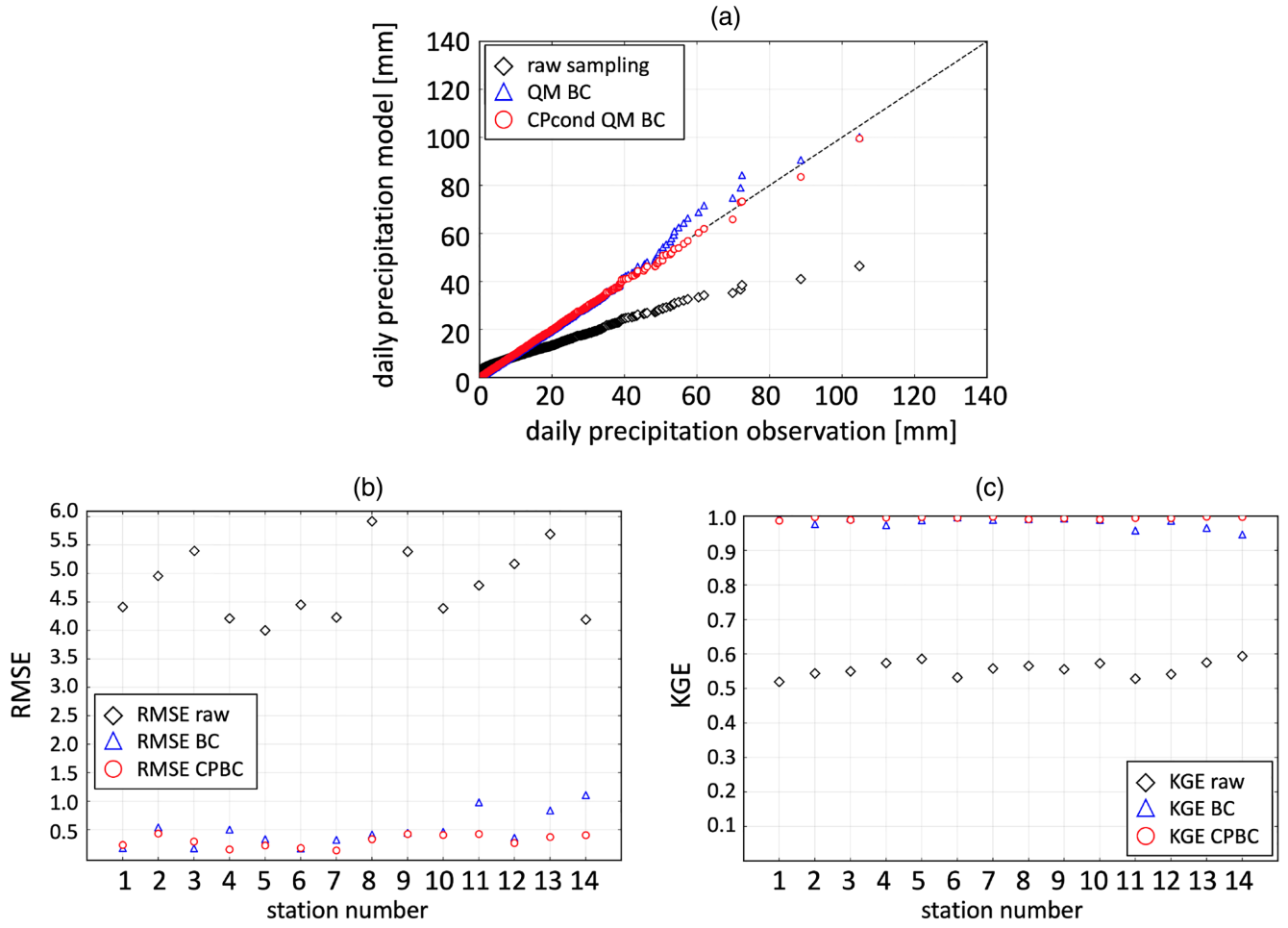

FIGURE 8 Observation-model plot of the resampled training period precipitation at Garmisch-Partenkirchen station (a). Real mean squared error (b) and Kling–Gupta efficiency (c) of the resampled precipitation at the used 14 stations. Black diamonds indicate uncorrected model output, blue triangles corrected model output by standard method, and red circles CP conditional corrected model output.

5, and CP 7 are of special interest. While CP 3 has an occurrence probability in the training period of 4.9% it was present during 20.9% of the 99th percentile precipitation days, CP 7 has an occurrence probability of 15.5% and was present during 39.5% of the 99th percentile precipitation days and CP 5 has an occurrence probability of 16.5% and was present during 27.9% of the 99th percentile precipitation days. Though heavy precipitation can also occur under other CPs, the formerly mentioned three CPs are the most relevant ones for heavy precipitation events, explaining 88.3% of the 99th percentile precipitation days. Therefore changes in the occurrence of these CPs as described in subsequent sections are of special importance for heavy precipitation.

4.1.2 | CDFs of CPs

Investigating the discriminative power of the created classification on precipitation at a specific location the CP-wise CDFs of each station are derived. Figure 5 shows the derived CDFs for one station, and in Figure A2 the other stations are shown. CPs yielding less precipitation relative to the stations reference CDF and CPs yielding more precipitation relative to the reference can clearly be distinguished. CP 6 can be considered the driest class and CP 4 and CP 1 as moderately drier than the reference. CP 7 and CP 3 are the wettest classes relative to the reference. The precipitation distributions of CP 2 and CP 5 can be considered closely to reflect the reference distribution.

4.1.3 | Frequency changes of CPs

Investigating the derived classification catalogues for the presence of occurrence frequency changes of CPs yields the trend lines shown in Figure 6. Analysing a 35 years time series frequency changes can be observed in five out of seven CPs. Of particular interest are frequency changes of the CPs which have CDFs very different from the reference CDF. Therefore the observed frequency change of CP 7 (g in Figure 6) must be highlighted. This frequency change is not only increasing but the only one being statistically significant passing the Mann-Kendall test at the 95% confidence level. This increasing occurrence of CP

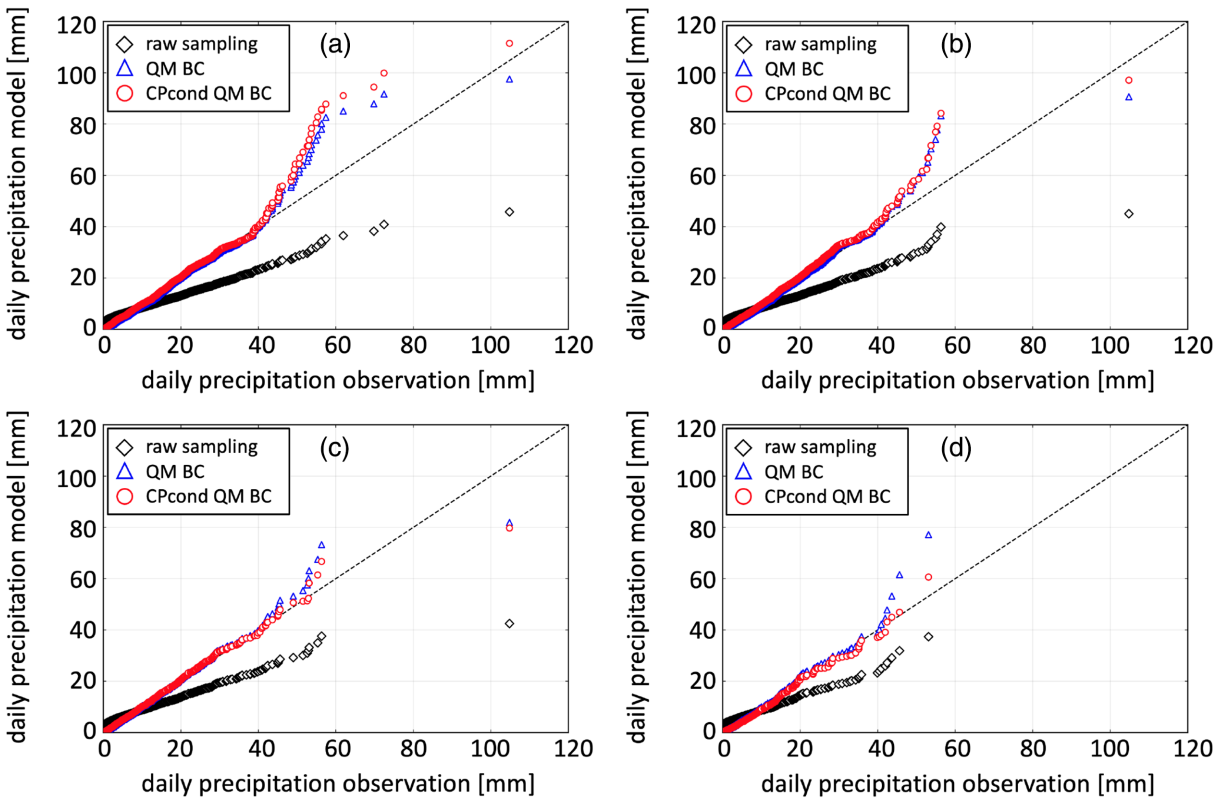

FIGURE 9 Observation-model plots with varying lengths of the training and sampling period. Starting from a 5 years training period (a) to 15 years (b), to 25 years (c) and 35 years (d) respectively. Black diamonds indicate uncorrected model output, blue triangles corrected model output by the standard method, and red circles CP conditional corrected model output.

7 is mostly at the expense of the occurrence of CP 6 and CP 4 (in Figure 6f,d).

4.2 | Bias correction

4.2.1 | Predictor choice

Testing different predictors in the classifications it can be observed that in general, all tested classifications are skillful (Figure 7). Nevertheless, some predictor combinations appear to be slightly more stable in yielding good correction results at all stations. Said predictors are mean sea level pressure and the combination of mean sea level pressure together with the 10-m u- and v-wind components which perform equally well. A combination of mean sea level pressure and geopotential at 500 hPa occasionally has a higher skill in terms of Kling–Gupta efficiency (station 12) but yields a larger spread over all stations. Though the choice of different additional predictors other than mean sea level pressure can improve the resulting skill it can clearly be stated that mean sea level pressure is the single most important predictor. Compared to the approach using Hess–Brezowsky general circulation patterns, mean sea level pressure and mean sea level pressure together with the 10-m u- and v-wind component yield an equal performance using 7 semi-objective CPs. The approach with geopotential at 500 hPa as the second predictor is not as stable as the Hess–Brezowsky approach.

4.2.2 | Resampling of training period

Analysing the performance in reproducing the precipitation distributions of the training period it can be stated that all used bias correction methods in general yield satisfying results. However, in terms of RMSE and KGE gains the circulation pattern conditional correction approach outperforms standard statistical correction methods for most stations and shows more stable improvement characteristics in between stations (Figure 8). These findings support the assumption that the conservation and utilization of atmospheric information through the classification can lead to a more reliable statistical downscaling of precipitation.

4.2.3 | Length of training period

It can be observed that the performance in representing the distribution of the measured precipitation at a

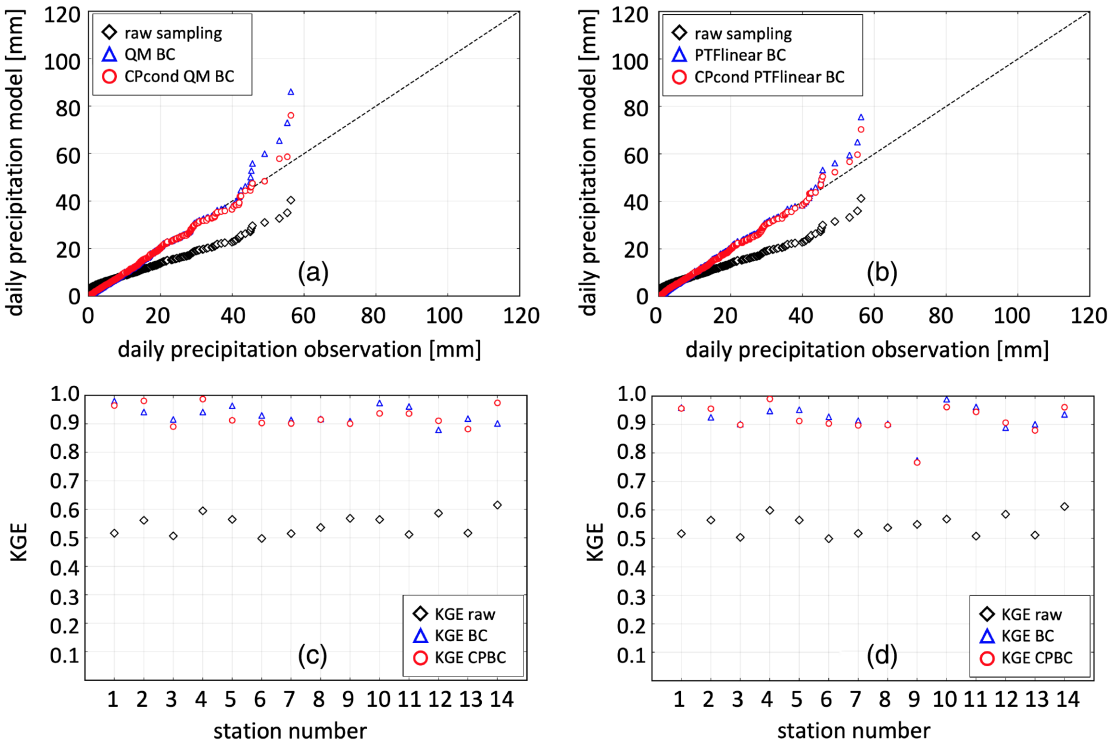

FIGURE 10 Observation-model plots at the Garmisch-Partenkirchen station for quantile mapping (a) and linear parametric transformation function (b) as correction method. Kling–Gupta efficiency at all stations for quantile mapping (c) and linear parametric transformation function (d). Black diamonds indicate uncorrected model output, blue triangles corrected model output by the standard method, and red circles CP conditional corrected model output.

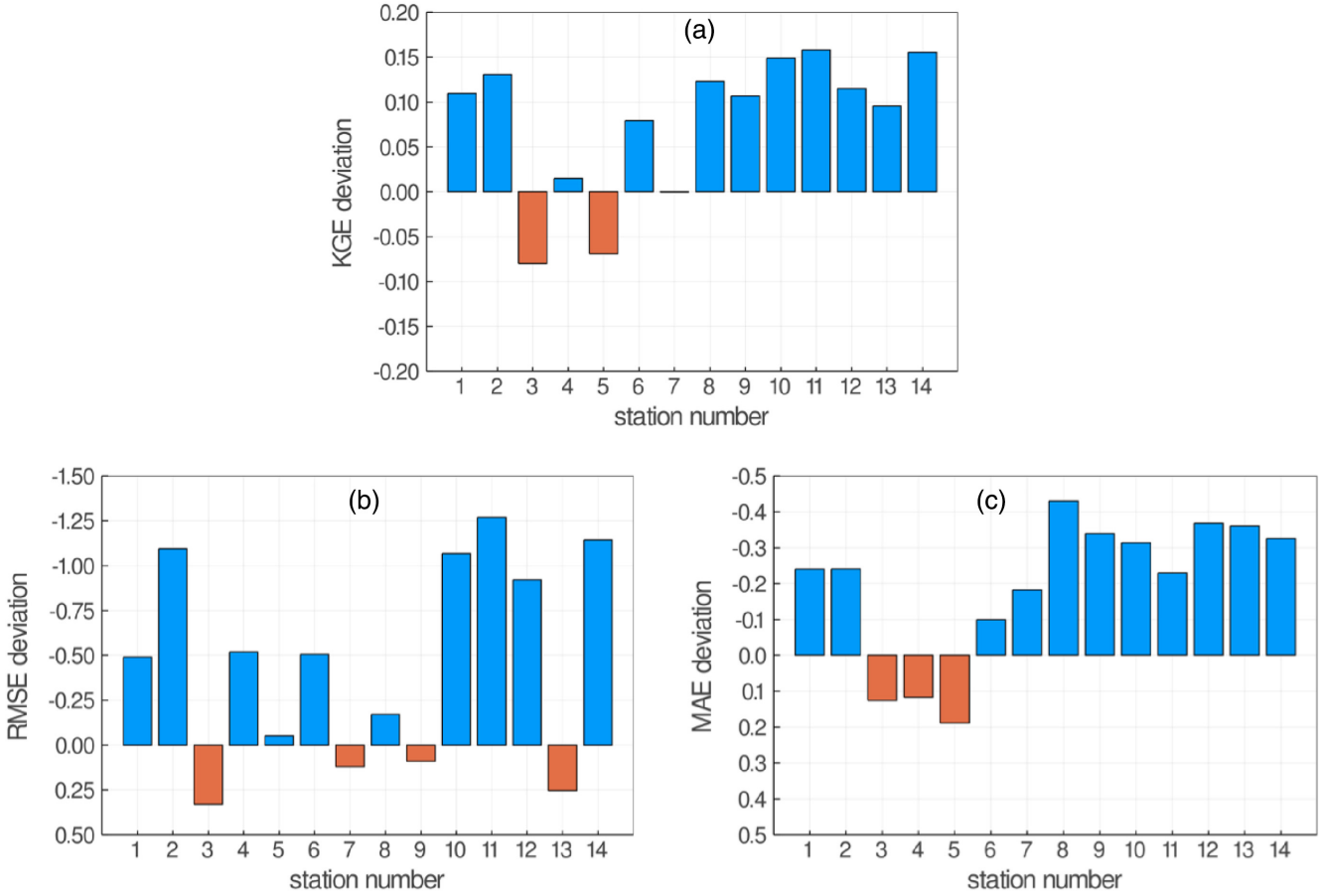

FIGURE 11 Kling–Gupta efficiency (a), RMSE (b) and MAE (c) deviation between standard bias corrected modelled precipitation and CP conditional corrected model precipitation for the complete distribution at all stations. Negative values on the inverted y-axis indicate performance gains of the CP conditional corrected model precipitation, and positive values indicate losses.

specific site is improved the longer the available training dataset gets. This remains true for all bias correction approaches used. For most of the stations, the results show that quantile mapping correction using all the data of the given training period at once outperforms CP-conditioned correction in the case of short training periods. Though the longer the training periods get the more likely it is that CP-conditioned bias correction yields better agreement to the measured precipitation distribution. These characteristics are shown in Figure 9 in an exemplary way for the Garmisch-Partenkirchen station.

4.2.4 | Bias correction method

Both tested bias correction methods, non-parametric empirical quantile transformation, and a linear parametric transformation function are equally capable of improving the skill of correcting the precipitation distributions. Figure 10 shows these characteristics in an exemplary way for the Garmisch-Partenkirchen station. Though there are small differences in the resulting distributions the general shape remains the same. In terms of Kling–Gupta efficiency both methods perform comparably well with the non-parametric empirical quantile transformation being slightly more stable (Figure 10).

4.3 | Performance evaluation

4.3.1 | Complete distribution

Analysing the performance of correcting the complete precipitation distribution in the evaluation period, the standard bias correction approach and the CP conditional approach are capable of improving the raw model output significantly as shown in the previous section (Figure 10). The observation-model plots for all stations are shown in the Figure A3. Comparing the standard bias correction approach to the CP conditional approach it can be observed that, in general, the latter shows a better performance resulting in smaller MAE and RMSE and higher

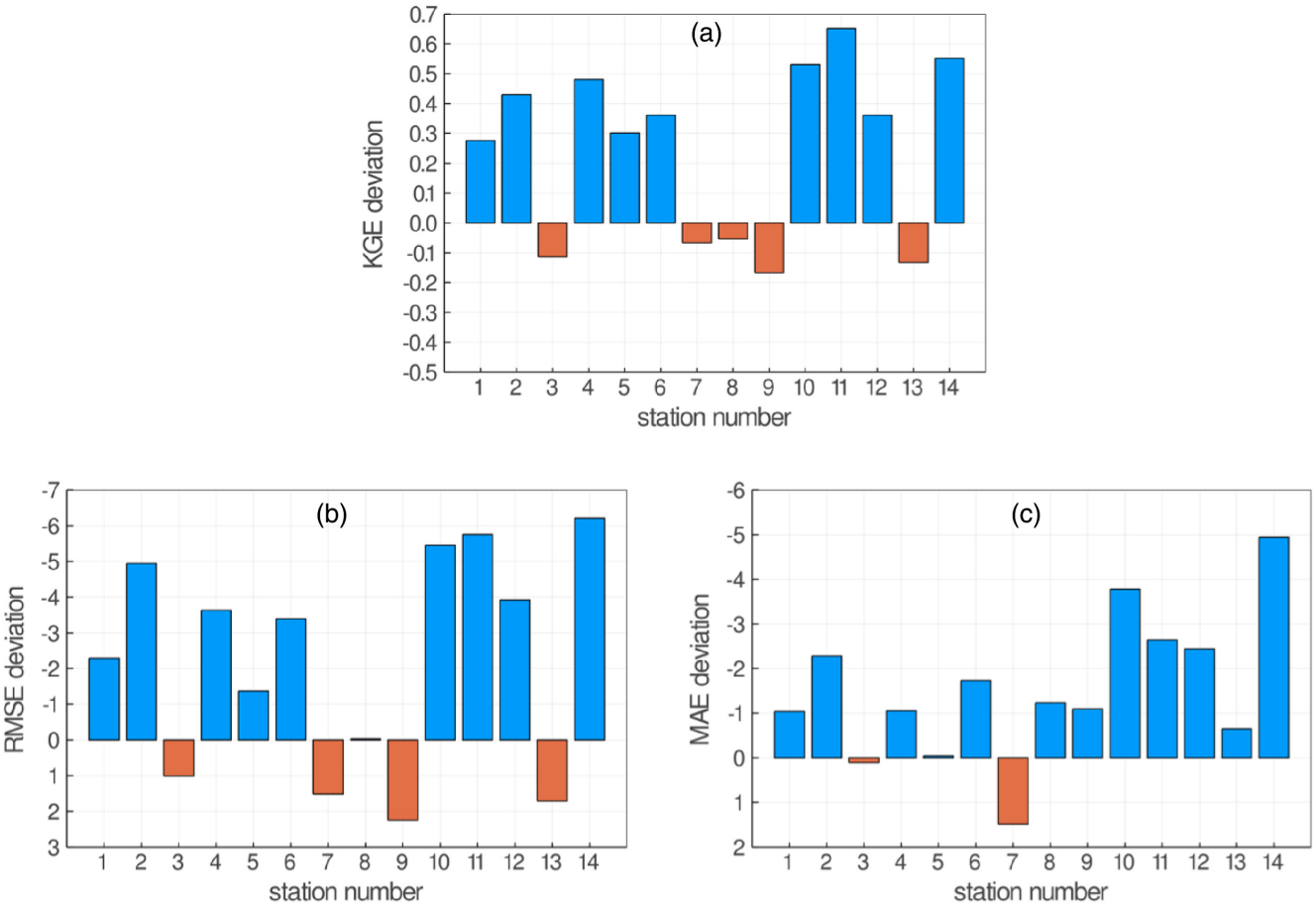

FIGURE 12 Kling–Gupta efficiency (a), RMSE (b) and MAE (c) deviation between standard bias corrected modelled precipitation and CP conditional corrected model precipitation for the 95th percentile and above at all stations. Negative values on the inverted y-axis indicate performance gains of the CP conditional corrected model precipitation, and positive values indicate losses.

KGE (Figure 11). However, there are notable exceptions to this for specific stations. These 'low performance' stations in terms of the CP conditional approach are either dependent on the used evaluation metric (stations 4, 5, 7, 9, and 13) or the CP conditional approach's performance is always lower than the standard approach's independent of the used metric (station 3). Taking into account that the absolute differences between the performances of the compared approaches are often marginal (e.g. RMSE at station 5 or KGE at stations 4 and 7) the results concerning the performance of correcting the complete distribution show that both approaches are equally skillful in doing so.

4.3.2 | Extremes

As the special focus of this study is on the extremes, Figure 12 shows the performance of the analysed approaches taking only the corrected distribution of the 95th percentile and higher into consideration. As for the correction performance of the complete distribution, there are some notable exceptions to the generally superior performance of the CP conditional approach. However, these exceptions are fewer (stations 5, 7, 9, and 13 dependent on the metric and 3 independent on the metric) and the performance gain can be much higher. Additionally, in terms of KGE the performance of the CP conditional approach on correcting the extremes is of higher average and more stable over all stations. Therefore, the evaluation results show that the correction performance of the CP conditional approach on correcting the extremes is generally superior to the standard approach and can yield significant improvements. An overview of the spatial distribution of KGE gains and losses for the complete distribution and the extremes is given in Figure 13.

5 | DISCUSSION

The conducted analyses show that the utilization of simple circulation patterns provides benefits to the results of

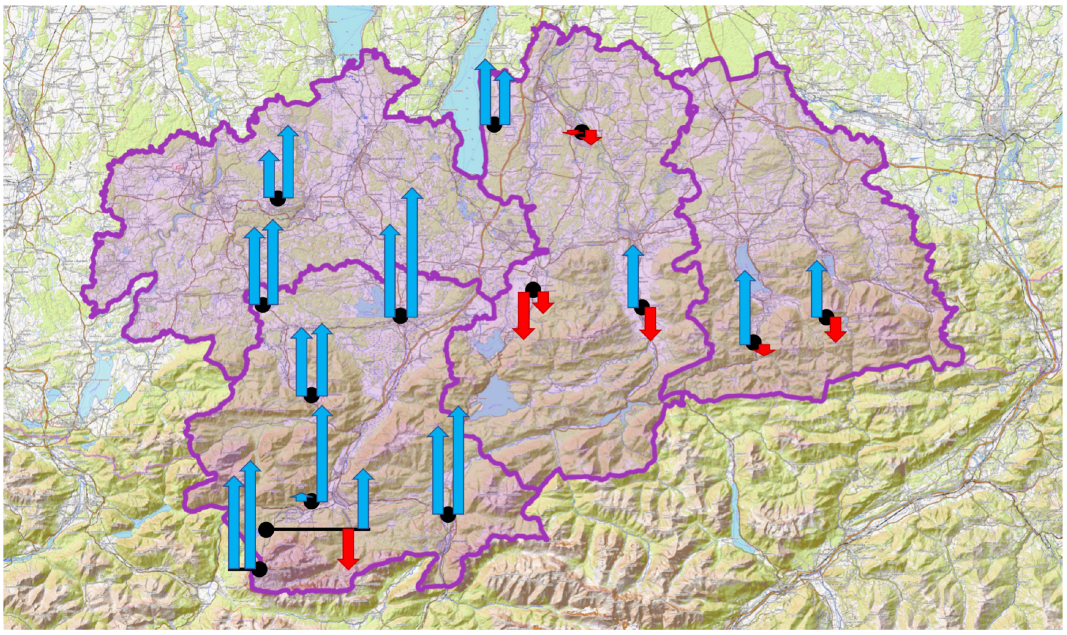

FIGURE 13 Spatial distribution of Kling–Gupta efficiency gains and losses for the complete distribution (arrows on the left-hand side of each station marker) and the 95th percentile (arrows on the right-hand side of each station marker). Blue arrows indicate performance gains, red arrows indicate performance losses of the CP conditional approach compared to the standard correction approach. Please note, left-hand side arrows and right-hand side arrows do not have the same scale. For actual values see Figures 11 and 12.

precipitation downscaling which is consistent with the findings described in (e.g. Bárdossy & Pegram, 2011; Yang et al., 2010). This holds true even though we followed a strict 'circulation to environment' approach of not taking precipitation into account for the classification itself, which differs from the approach used in Bárdossy and Pegram (2011) and the development of the corresponding classification described in Bárdossy (2010). The creation of sets of CDFs of CPs for the sampling process expands its range of likely values giving the sampling process higher probabilities of picking more extreme values under certain physically based (CPs) conditions. This assumed advantage of a greater range for precipitation sampling is backed by the findings of our study in which the performance gain in reflecting the 95th percentile and above for certain stations in terms of KGE reached values up to +0.6. Results show that there are frequency changes present in the occurrence of CPs during the training period having an increasing occurrence probability of CP 5 and CP 7 which are found to be linked to heavy precipitation events occurring in the study region. Combining the latter two findings the CP conditional approach's superior performance, especially in the extremes confirms the validity of the assumptions presented in the introduction section. Meaning that the conservation of frequency changes in the occurrence of atmospheric states and the discriminative power of CPs on precipitation is indeed beneficial to the downscaling results compared to the tested standard approaches. These characteristics of 'circulation to environment' CPs having discriminative power with respect to precipitation have also been described by (e.g. Laux et al., 2020; Mehrotra et al., 2004).

Nevertheless, the results also show that the presented CP conditional approach inherits characteristics and limitations that need to be discussed and should furthermore be assessed in detail and addressed as necessary in the future. Known factors that may influence the outcome of the downscaling process are residing around the circulation patterns classification itself. One crucial decision that has to be made in advance of the clustering is the number of clusters to be created. In the case of this study the number of clusters has been determined by stating that an explained cluster variance above 0.8 is satisfying for the pursued purpose since the aim is not to create the best possible representation of the atmospheric state but to show that a simple set of circulation patterns provides discriminative power to precipitation and can potentially be used for downscaling which has been shown by Laux et al. (2020). Therefore basing the number of clusters on a subjective ECV threshold instead of utilizing one of the various methods for cluster number determination, for example, silhouette index or comparable metrics seems valid but leads to the fact that another number of clusters may lead to different results. Our findings show that the tested range of the number of clusters allows only for

slight differences in the results in terms of downscaling precipitation performance. This is consistent with the findings of Prudhomme and Genevier (2011) who state that the number of clusters is of lesser importance than the used algorithm. The used SANDRA algorithm however is confirmed as showing reliable and good clustering performance by various studies (e.g. Huth et al., 2008; Kučerová et al., 2017; Philipp et al., 2007; Philipp et al., 2016; Prudhomme & Genevier, 2011) which is in good agreement with the achieved high ECVs (Figure A3) in our study. This leaves the selection of predictors as most influential to the suitability of a classification for a given station to be downscaled as described in the corresponding section. This selection has been conducted in a way that predictors have been chosen which have been identified as important for precipitation by other studies. For the utilization of said predictors for downscaling and future predictions the assumption of temporally stationary correlations of the circulation and precipitation holds true to what has been described for our most dominant predictor MSLP in Wilby and Wigley (2000). Haberlandt et al. (2015) who evaluated critical assumptions considering CP conditional downscaling confirm a strong relationship between CPs and precipitation but reject the stationarity assumption clearly. Adding to the latter study Beck et al. (2007) and Jones and Lister (2009) state that the stationarity of these correlations may be questioned due to within-type variations. Due to these findings, we stress the selection of predictors taken into consideration and the link between CPs and precipitation needs to be evaluated frequently. Additionally, the downscaling method proposed needs to be extended to account for such non-stationarities if used for long-term predictions.

In addition to the classification-related characteristics, three other influences should be discussed. First in terms of bias correction method selection, our findings have good agreement with the statements in Gudmundsson et al. (2012) that non-parametric correction methods like the tested empirical quantile mapping are more reliable than methods using parametric transfer functions so the conducted focusing on the former can be considered appropriate for this type of downscaling precipitation. Despite this finding, it may be necessary to create ensembles including different (CP conditional) bias correction approaches to utilize the proposed methods for impact studies due to influences of bias correction method selection as shown by Laux et al. (2021b). Second, the used bias correction method does not account for trends present in the precipitation time series itself. Since the focus of our study is mainly on the conservation of frequency changes of CPs we decided to omit testing methods capable of precipitation trend conservation in order to avoid potential interference between CP frequency changes and precipitation trends. Nevertheless, it must be noted that precipitation trend-preserving methods like quantile delta mapping proposed by (Cannon et al., 2015) or trend-preserving bias adjustment described by (Lange, 2019) may improve the method's reliability even further. Thirdly there are the characteristics of the performance evaluation metrics themselves. As stated in Chai and Draxler (2014) MAE and RMSE give different types of errors and different weights resulting in the RMSE being much more sensitive to a single outlier than the MAE. We observed this characteristic, especially for the evaluation of the representation of extremes where for example at station 9 the CP conditional approach performs better in terms of KGE and MAE but not in terms of RMSE which can be explained by the presence of a single outlier. So the variance of performance can partly be explained by the selection of the evaluation metric. Our findings, therefore, support the suggestion that more than one metric should be provided in the evaluation process (e.g. Chai & Draxler, 2014; Laux et al., 2021a).

6 | SUMMARY AND CONCLUSION

The results of this study show that the proposed method of CP conditional downscaling is able to yield more reliable precipitation distributions even more so for the extremes compared to the tested standard approaches. Being aware of the discussed characteristics and limitations we conclude that the presented method of CP conditional downscaling provides an added value to the reliability of daily precipitation prediction in the complex terrain study region. Since the same bias correction is applied to the CP conditional and the non-CP conditional case the observed added value can only be attributed to the CP conditioning. Due to the strict 'circulation to environment' approach the identified CPs can easily be assigned to climate model output and used for future predictions. The presented method inherits potential for future extensions overcoming existing limitations. The stationarity assumption described above is one of the most important limitations to dealing with the implementation of a delta change approach taking the change from RCM simulations and applying it for parameter re-estimation of the precipitation modelling as proposed by Haberlandt et al. (2015) may be an appropriate extension. Other approaches such as including the temperature as an additional predictor of the classification as conducted by Beck and Bárdossy (2013) might be a suitable solution, too. Additionally, we emphasize the option of transferring this approach to grid-based downscaling and to a sub-daily scale in the future. The former can be accomplished by

using gridded radar precipitation observations and gives the opportunity of being able to downscale to the area rather than just to specific points dependent on the position of the stations available. Expanding the approach to the sub-daily scale which can potentially also be accomplished by using radar observations provides a solution to the limitation of not being able to really distinguish heavy precipitation events from longer-lasting rain events on the daily scale. This opens up the opportunity to train the presented downscaling method even more specifically to the type of event desired and advancing it to a level it can be used for reliable heavy precipitation prediction-based planning of climate change adaption measures.

AUTHOR CONTRIBUTIONS

Brian Böker: Conceptualization; methodology; software; data curation; investigation; validation; formal analysis; visualization; resources; writing – original draft; writing – review and editing. **Patrick Laux:** Conceptualization; data curation; supervision; funding acquisition; project administration; writing – review and editing. **Patrick Olschewski:** Methodology; software; writing – review and editing; visualization. **Harald Kunstmann:** Supervision.

ACKNOWLEDGEMENTS

The majority of this analysis was performed using the cost733class software package (Philipp et al., 2014) for clustering and the programming language Julia, version 1.7 (Bezanson et al., 2017) for the rest. In addition, the R package 'qmap' (Gudmundsson et al., 2012) was consulted for the correction of bias. We acknowledge the provision of DWD station data and ERA5 data that was used in this study. Open Access funding enabled and organized by Projekt DEAL.

CONFLICT OF INTEREST STATEMENT

The authors declare no competing interests.

DATA AVAILABILITY STATEMENT

The used ERA5 reanalysis data is openly accessible via the Climate Data Store of the European Centre for Medium-Range Weather Forecasts (ECMWF) under the following link: https://cds.climate.copernicus.eu/cdsapp#!/dataset/reanalysis-era5-pressure-levels?tab=overview. The used station data of the German Weather Service (DWD) is openly accessible via its Climate Data Center under the following link: https://cdc.dwd.de/portal/.

ORCID

Brian Böker https://orcid.org/0000-0001-9539-3385
Patrick Laux https://orcid.org/0000-0002-8657-6152

REFERENCES

Bárdossy, A. (2010) Atmospheric circulation pattern classification for South-West Germany using hydrological variables. *Physics and Chemistry of the Earth*, 35(9–12), 498–506. Available from: https://doi.org/10.1016/j.pce.2010.02.007

Bárdossy, A. & Pegram, G. (2011) Downscaling precipitation using regional climate models and circulation patterns toward hydrology. *Water Resources Research*, 47(4), 4505. Available from: https://doi.org/10.1029/2010WR009689

Beck, C., Jacobeit, J. & Jones, P.D. (2007) Frequency and within-type variations of large-scale circulation types and their effects on low-frequency climate variability in central europe since 1780. *International Journal of Climatology*, 27(4), 473–491. Available from: https://doi.org/10.1002/joc.1410

Beck, F. & Bárdossy, A. (2013) Indirect downscaling of global circulation model data based on atmospheric circulation and temperature for projections of future precipitation in hourly resolution. *Hydrology and Earth System Sciences Discussions*, 10(7), 8841–8874. Available from: https://doi.org/10.5194/hessd-10-8841-2013

Bezanson, J., Edelman, A., Karpinski, S. & Shah, V.B. (2017) Julia: a fresh approach to numerical computing. *SIAM Review*, 59(1), 65–98. Available from: https://doi.org/10.1137/141000671

Boé, J., Terray, L., Habets, F. & Martin, E. (2007) Statistical and dynamical downscaling of the Seine basin climate for hydro-meteorological studies. *International Journal of Climatology*, 27(12), 1643–1655. Available from: https://doi.org/10.1002/joc.1602

Cannon, A.J., Sobie, S.R. & Murdock, T.Q. (2015) Bias correction of GCM precipitation by quantile mapping: how well do methods preserve changes in quantiles and extremes? *Journal of Climate*, 28(17), 6938–6959. Available from: https://doi.org/10.1175/JCLI-D-14-00754.1

Chai, T. & Draxler, R.R. (2014) Root mean square error (RMSE) or mean absolute error (MAE)?—Arguments against avoiding RMSE in the literature. *Geoscientific Model Development*, 7, 1247–1250. Available from: https://doi.org/10.5194/gmd-7-1247-2014

Dayan, U., Tubi, A. & Levy, I. (2012) On the importance of synoptic classification methods with respect to environmental phenomena. *International Journal of Climatology*, 32(5), 681–694. Available from: https://doi.org/10.1002/joc.2297

Demuzere, M., Werner, M., van Lipzig, N.P.M. & Roeckner, E. (2009) An analysis of present and future ECHAM5 pressure fields using a classification of circulation patterns. *International Journal of Climatology*, 29(12), 1796–1810. Available from: https://doi.org/10.1002/joc.1821

Deumlich, D. & Gericke, A. (2020) Frequency trend analysis of heavy rainfall days for Germany. *Water*, 12(7), 1950. Available from: https://doi.org/10.3390/w12071950

Deutscher Wetterdienst. (2022) Climate Data Center. https://cdc.dwd.de/portal/

Eden, J.M., Widmann, M., Grawe, D. & Rast, S. (2012) Skill, correction, and downscaling of GCM-simulated precipitation. *Journal of Climate*, 25(11), 3970–3984. Available from: https://doi.org/10.1175/JCLI-D-11-00254.1

ESWD. (2022) Heavy rainfall map Germany 1950–2021. https://www.eswd.eu/cgi-bin/eswd.cgi?lang=en0&lastquery=9435332817&forcedynamicmap=true

Faranda, D., Vrac, M., Yiou, P., Jézéquel, A. & Thao, S. (2020) Changes in future synoptic circulation patterns: consequences for extreme event attribution. *Geophysical Research Letters*, 47(15), 1–9. Available from: https://doi.org/10.1029/2020GL088002

Gerstengarbe, F.W. & Werner, P.C. (2005) Katalog der grosswetterlagen Europas (1881–2004): Nach Paul Hess und Helmut Brezowsky 6., verbesserte und ergänzte auflage. *PIK Report*, 100, 1–148.

Giorgi, F., Jones, C. & Asrar, G.R. (2009) Addressing climate information needs at the regional level: the CORDEX framework. Tech. Rep. 3. http://wcrp.ipsl

Grieser, J., Beck, C. & Rudolf, B. (2006) The Summer Flooding 2005 in Southern Bavaria—A Climatological Review. Tech. rep., DWD. https://www.dwd.de/DE/leistungen/klimastatusbericht/publikationen/ksb2005pdf/162005.pdf;jsessionid=76CD26D3E62A49C59542D19F9944EE87.live21061?blob=publicationFile&v=1

Gudmundsson, L., Bremnes, J.B., Haugen, J.E. & Engen-Skaugen, T. (2012) Technical note: downscaling RCM precipitation to the station scale using statistical transformations—a comparison of methods. *Hydrology and Earth System Sciences*, 16(9), 3383–3390. Available from: https://doi.org/10.5194/hess-16-3383-2012

Gupta, H.V., Kling, H., Yilmaz, K.K. & Martinez, G.F. (2009) Decomposition of the mean squared error and NSE performance criteria: implications for improving hydrological modelling. *Journal of Hydrology*, 377(1–2), 80–91. Available from: https://doi.org/10.1016/j.jhydrol.2009.08.003

Haberlandt, U., Belli, A. & Bárdossy, A. (2015) Statistical downscaling of precipitation using a stochastic rainfall model conditioned on circulation patterns—an evaluation of assumptions. *International Journal of Climatology*, 35(3), 417–432. Available from: https://doi.org/10.1002/joc.3989

Hersbach, H., Bell, B., Berrisford, P., Hirahara, S., Horányi, A., Muñoz-Sabater, J. et al. (2020) The ERA5 global reanalysis. *Quarterly Journal of the Royal Meteorological Society*, 146(730), 1999–2049. Available from: https://doi.org/10.1002/qj.3803

Horton, D.E., Johnson, N.C., Singh, D., Swain, D.L., Rajaratnam, B. & Diffenbaugh, N.S. (2015) Contribution of changes in atmospheric circulation patterns to extreme temperature trends. *Nature*, 522(7557), 465–469. Available from: https://doi.org/10.1038/nature14550

Huth, R., Beck, C., Philipp, A., Demuzere, M., Ustrnul, Z., Cahynová, M. et al. (2008) Classifications of atmospheric circulation patterns recent advances and applications. *Trends and Directions in Climate Research*, 1146(1), 105–152. Available from: https://doi.org/10.1196/annals.1446.019

Ibebuchi, C.C. (2022) Patterns of atmospheric circulation in Western Europe linked to heavy rainfall in Germany: preliminary analysis into the 2021 heavy rainfall episode. *Theoretical and Applied Climatology*, 148(1–2), 269–283. Available from: https://doi.org/10.1007/s00704-022-03945-5

Ibebuchi, C.C. (2023) On the representation of atmospheric circulation modes in regional climate models over Western Europe. *International Journal of Climatology*, 43(1), 668–682. Available from: https://doi.org/10.1002/joc.7807

IPCC. (2021) Climate change 2021: the physical science basis. In: *Contribution of Working Group I to the Sixth Assessment Report of the Intergovernmental Panel on Climate Change*. Cambridge University Press, Cambridge.

Jacobeit, J., Homann, M., Philipp, A. & Beck, C. (2017) Atmospheric circulation types and extreme areal precipitation in southern Central Europe. *Advances in Science and Research*, 14, 71–75. Available from: https://doi.org/10.5194/asr-14-71-2017

Jones, P.D. & Lister, D.H. (2009) The influence of the circulation on surface temperature and precipitation patterns over Europe. *Climate of the Past*, 5(2), 259–267. Available from: https://doi.org/10.5194/cp-5-259-2009

Kilsby, C.G., Jones, P.D., Burton, A., Ford, A.C., Fowler, H.J., Harpham, C. et al. (2007) A daily weather generator for use in climate change studies. *Environmental Modelling and Software*, 22(12), 1705–1719. Available from: https://doi.org/10.1016/j.envsoft.2007.02.005

Knoben, W.J., Freer, J.E. & Woods, R.A. (2019) Technical note: inherent benchmark or not? Comparing Nash–Sutcliffe and Kling–Gupta efficiency scores. *Hydrology and Earth System Sciences*, 23(10), 4323–4331. Available from: https://doi.org/10.5194/hess-23-4323-2019

Kučerová, M., Beck, C., Philipp, A. & Huth, R. (2017) Trends in frequency and persistence of atmospheric circulation types over Europe derived from a multitude of classifications. *International Journal of Climatology*, 37(5), 2502–2521. Available from: https://doi.org/10.1002/joc.4861

Lange, S. (2019) Trend-preserving bias adjustment and statistical downscaling with ISIMIP3BASD (v1.0). *Geoscientific Model Development*, 12(7), 3055–3070. Available from: https://doi.org/10.5194/gmd-12-3055-2019

Laux, P., Böker, B., Martins, E.S., Vasconcelos Junior, F., Moron, V., Portele, T. et al. (2020) A semi-objective circulation pattern classification scheme for the semi-arid Northeast Brazil. *International Journal of Climatology*, 41, 51–72. Available from: https://doi.org/10.1002/joc.6608

Laux, P., Dieng, D., Portele, T.C., Wei, J., Shang, S., Zhang, Z. et al. (2021a) A high-resolution regional climate model physics ensemble for northern sub-Saharan Africa. *Frontiers in Earth Science*, 9(9), 1–16. Available from: https://doi.org/10.3389/feart.2021.700249

Laux, P., Rötter, R.P., Webber, H., Dieng, D., Rahimi, J., Wei, J. et al. (2021b) To bias correct or not to bias correct? An agricultural impact modelers' perspective on regional climate model data. *Agricultural and Forest Meteorology*, 304–305, 108406. Available from: https://doi.org/10.1016/j.agrformet.2021.108406

Liu, M., Bárdossy, A. & Zehe, E. (2013) Interaction of valleys and circulation patterns (CPs) on spatial precipitation patterns in southern Germany. *Hydrology and Earth System Sciences*, 17, 4685–4699. Available from: https://doi.org/10.5194/hess-17-4685-2013

Liu, Y., Zhang, W., Shao, Y., Kexin, Z., Liu, C., Zhang, W.C. et al. (2011) A comparison of four precipitation distribution models used in daily stochastic models. *Advances in Atmospheric Sciences*, 28(4), 809–820. Available from: https://doi.org/10.1007/s00376

Lutz, K., Jacobeit, J., Philipp, A., Seubert, S., Kunstmann, H. & Laux, P. (2012) Comparison and evaluation of statistical downscaling techniques for station-based precipitation in the Middle East. *International Journal of Climatology*, 32(10), 1579–1595. Available from: https://doi.org/10.1002/joc.2381

Mahto, S.S. & Mishra, V. (2019) Does ERA-5 outperform other reanalysis products for hydrologic applications in India? *Journal of*

Geophysical Research: Atmospheres, 124(16), 9423–9441. Available from: https://doi.org/10.1029/2019JD031155

Maity, R., Suman, M., Laux, P. & Kunstmann, H. (2019) Bias correction of zero-inflated RCM precipitation fields: a copula-based scheme for both mean and extreme conditions. *Journal of Hydrometeorology*, 20(4), 595–611. Available from: https://doi.org/10.1175/JHM-D-18-0126.1

Mehrotra, R., Sharma, A. & Cordery, I. (2004) Comparison of two approaches for downscaling synoptic atmospheric patterns to multisite precipitation occurrence. *Journal of Geophysical Research D: Atmospheres*, 109(14), 1–15. Available from: https://doi.org/10.1029/2004JD004823

MunichRE. (2022) Natural disaster losses 2021. https://www.munichre.com/en/company/media-relations/media-information-and-corporate-news/media-information/2022/natural-disaster-losses-2021.html

Philipp, A., Beck, C., Huth, R. & Jacobeit, J. (2016) Development and comparison of circulation type classifications using the COST 733 dataset and software. *International Journal of Climatology*, 36(7), 2673–2691. Available from: https://doi.org/10.1002/joc.3920

Philipp, A., Beck, C. & Kreienkamp, F. (2014) COST733CLASS v1.2 user guide. https://www.researchgate.net/publication/269335894

Philipp, A., Della-Marta, P.M., Jacobeit, J., Fereday, D.R., Jones, P.D., Moberg, A. et al. (2007) Long-term variability of daily North Atlantic-European pressure patterns since 1850 classified by simulated annealing clustering. *Journal of Climate*, 20(16), 4065–4095. Available from: https://doi.org/10.1175/JCLI4175.1

Piani, C., Weedon, G.P., Best, M., Gomes, S.M., Viterbo, P., Hagemann, S. et al. (2010) Statistical bias correction of global simulated daily precipitation and temperature for the application of hydrological models. *Journal of Hydrology*, 395(3–4), 199–215. Available from: https://doi.org/10.1016/j.jhydrol.2010.10.024

Piper, D., Kunz, M., Ehmele, F., Mohr, S., Mühr, B., Kron, A. et al. (2016) Exceptional sequence of severe thunderstorms and related flash floods in May and June 2016 in Germany—part 1: meteorological background. *Natural Hazards and Earth System Sciences*, 16(12), 2835–2850. Available from: https://doi.org/10.5194/nhess-16-2835-2016

Prudhomme, C. & Genevier, M. (2011) Can atmospheric circulation be linked to flooding in Europe? *Hydrological Processes*, 25(7), 1180–1190. Available from: https://doi.org/10.1002/hyp.7879

Ramos, A.M., Barriopedro, D. & Dutra, E. (2015) Circulation weather types as a tool in atmospheric, climate, and environmental research. *Frontiers in Environmental Science*, 3(3), 1–3. Available from: https://doi.org/10.3389/fenvs.2015.00044

Rözer, V., Müller, M., Bubeck, P., Kienzler, S., Thieken, A., Pech, I. et al. (2016) Coping with pluvial floods by private households. *Water*, 8(7), 304. Available from: https://doi.org/10.3390/w8070304

Shepherd, T.G. (2014) Atmospheric circulation as a source of uncertainty in climate change projections. *Nature Publishing Group*, 7, 703–708. Available from: https://doi.org/10.1038/NGEO2253

Sunyer, M.A., Hundecha, Y., Lawrence, D., Madsen, H., Willems, P., Martinkova, M. et al. (2015) Inter-comparison of statistical downscaling methods for projection of extreme precipitation in Europe. *Hydrology and Earth System Sciences*, 19(4), 1827–1847. Available from: https://doi.org/10.5194/hess-19-1827-2015

Warscher, M., Wagner, S., Marke, T., Laux, P., Smiatek, G., Strasser, U. et al. (2019) A 5 km resolution regional climate simulation for Central Europe: performance in high mountain areas and seasonal, regional and elevation-dependent variations. *Atmosphere*, 10(11), 682. Available from: https://doi.org/10.3390/atmos10110682

Wilby, R.L. & Wigley, T.M. (2000) Precipitation predictors for downscaling: observed and general circulation model relationships. *International Journal of Climatology*, 20(6), 641–661. Available from: https://doi.org/10.1002/(SICI)1097-0088(200005)20:6⟨641::AID-JOC501⟩3.0.CO;2-1

Wilby, R.L., Wigley, T.M., Conway, D., Jones, P.D., Hewitson, B.C., Main, J. et al. (1998) Statistical downscaling of general circulation model output: a comparison of methods. *Water Resources Research*, 34(11), 2995–3008. Available from: https://doi.org/10.1029/98WR02577

Yang, W., Bárdossy, A. & Caspary, H.J. (2010) Downscaling daily precipitation time series using a combined circulation- and regression-based approach. *Theoretical and Applied Climatology*, 102(3), 439–454. Available from: https://doi.org/10.1007/s00704-010-0272-0

How to cite this article: Böker, B., Laux, P., Olschewski, P., & Kunstmann, H. (2023). Added value of an atmospheric circulation pattern-based statistical downscaling approach for daily precipitation distributions in complex terrain. *International Journal of Climatology*, *43*(11), 5130–5153. https://doi.org/10.1002/joc.8136

APPENDIX A

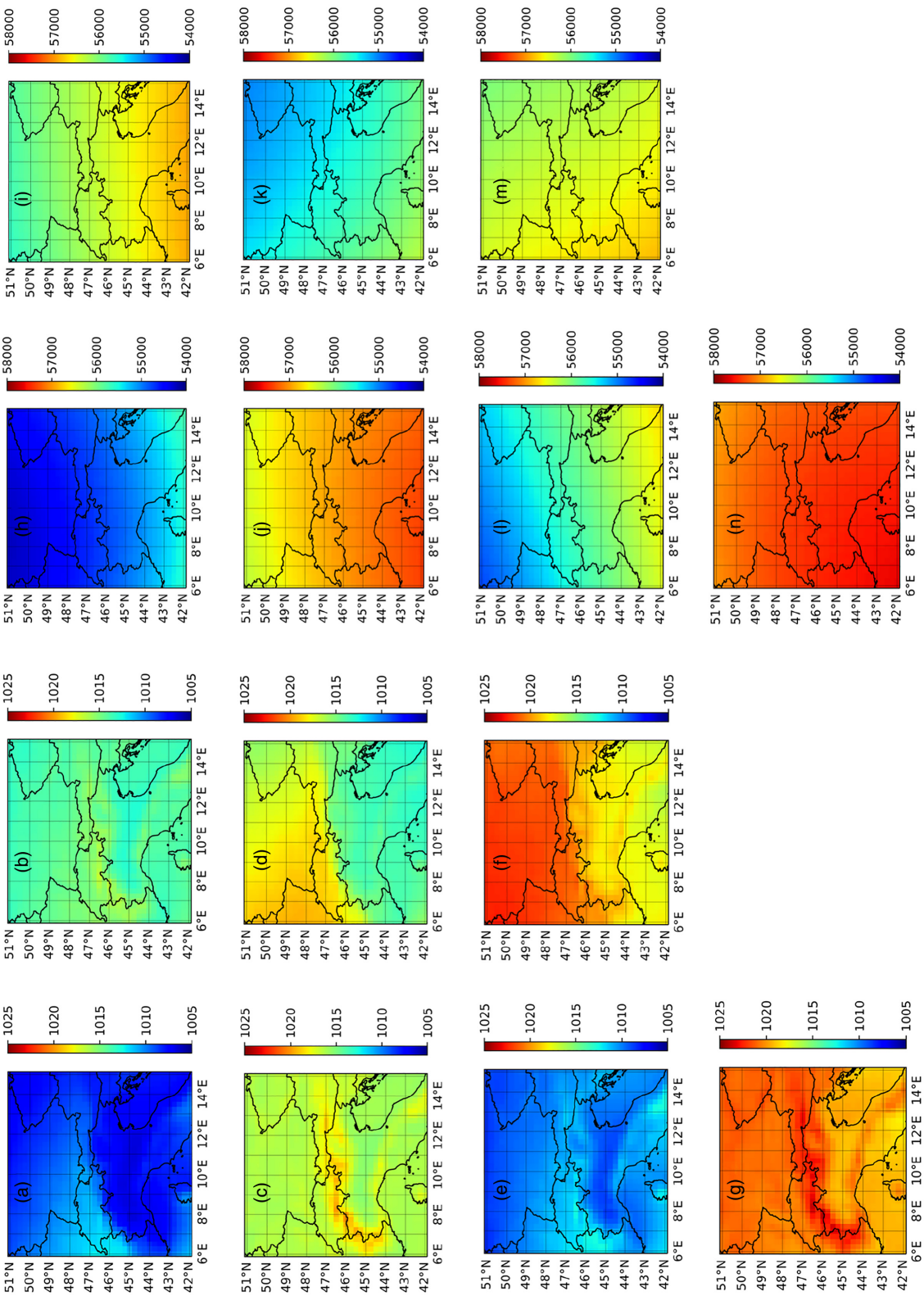

FIGURE A1 Mean sea level pressure (hPa) cluster centroids (a–g) and geopotential at the 500 hPa level ($m^2 \cdot s^{-2}$) cluster centroids (h–n) of a seven cluster solution based on mean sea level pressure and geopotential at 500 hPa level ERA 5 data. [Colour figure can be viewed at wileyonlinelibrary.com]

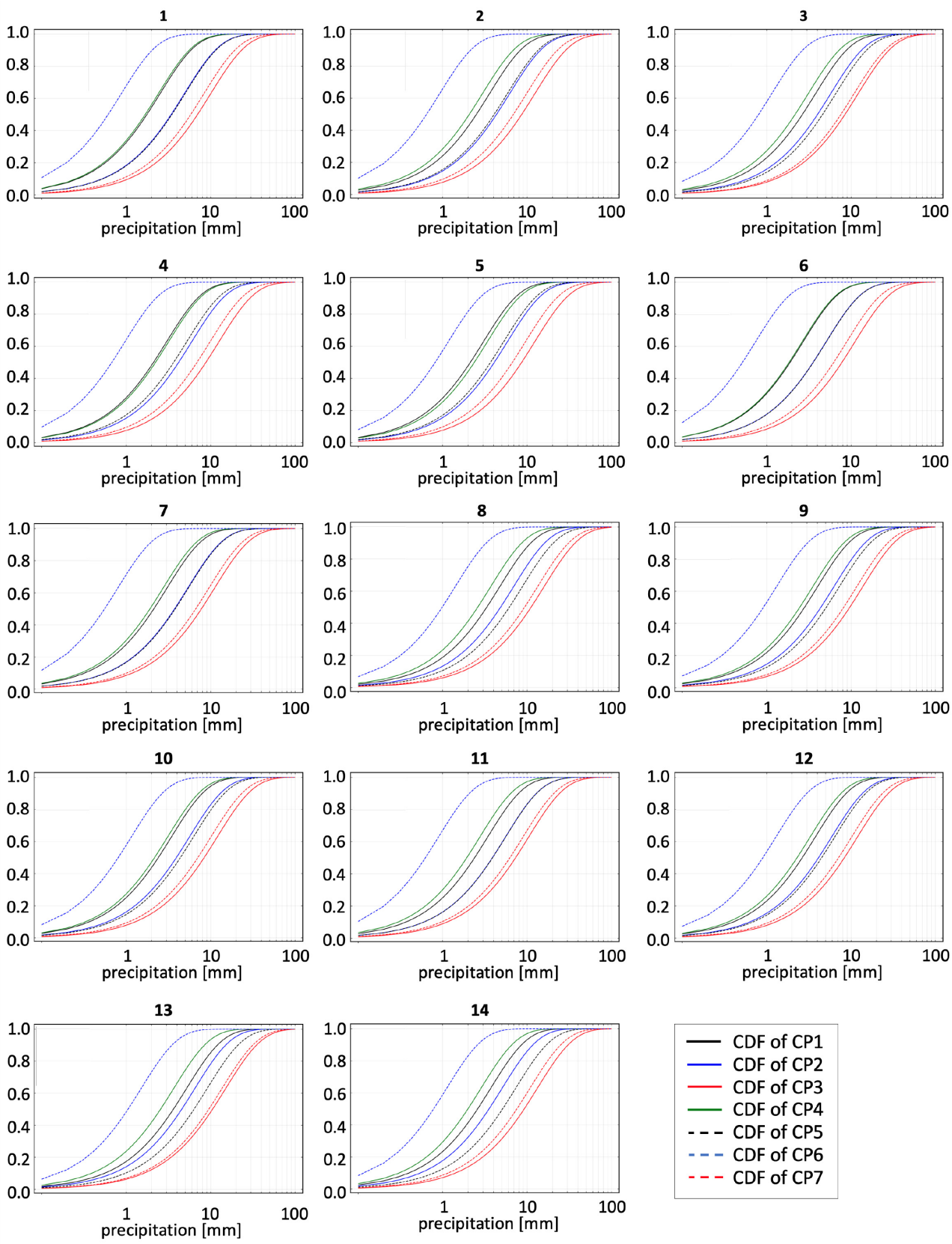

FIGURE A2 Cumulative distribution functions used for precipitation sampling of a seven cluster solution based on mean sea level pressure and u- and v-wind component at stations 1–14. [Colour figure can be viewed at wileyonlinelibrary.com]

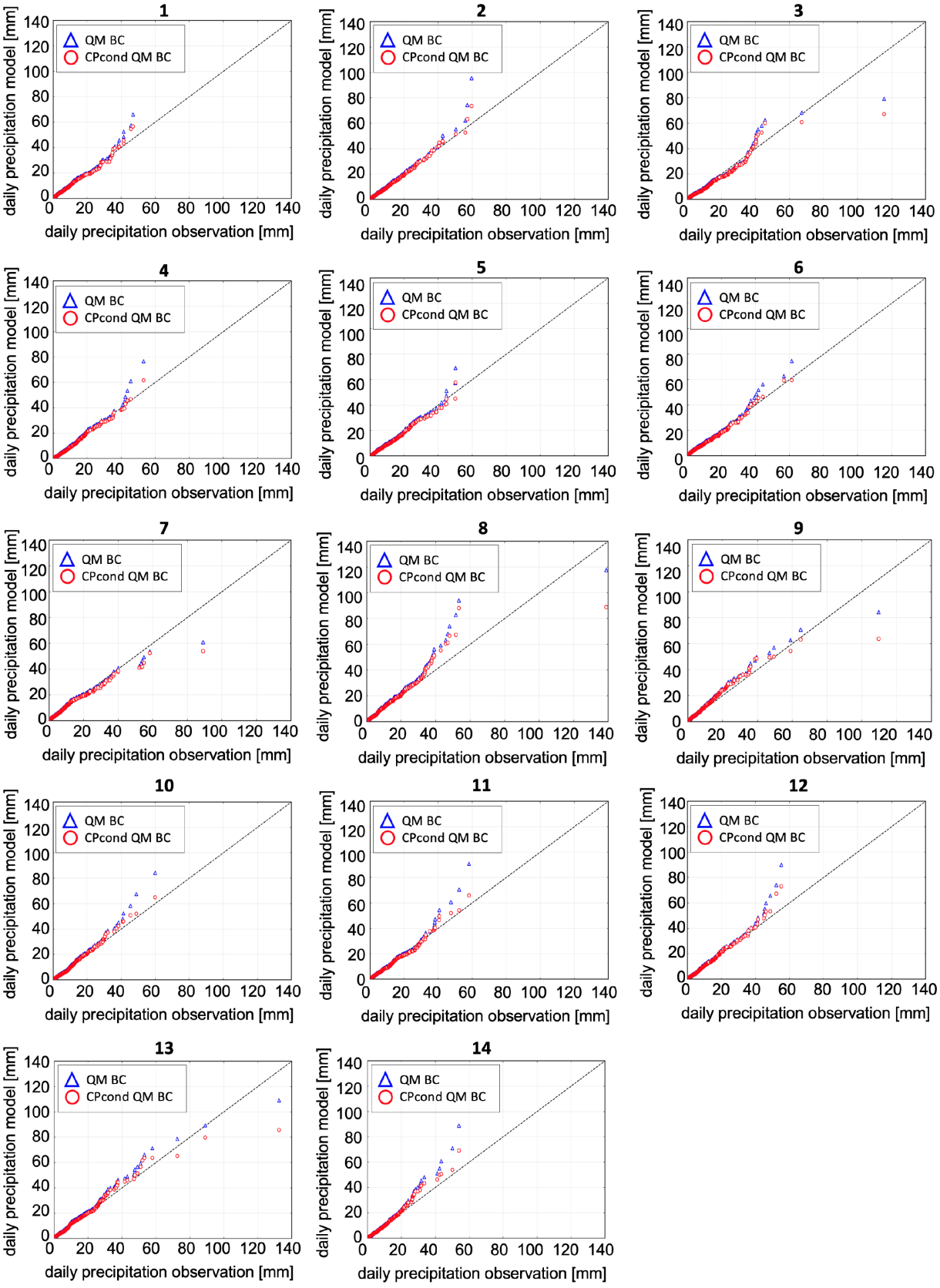

FIGURE A3 Observation-model plots for QM downscaled precipitation (blue triangles) and CP conditional QM downscaled (red circles) precipitation at station numbers 1–14. [Colour figure can be viewed at wileyonlinelibrary.com]